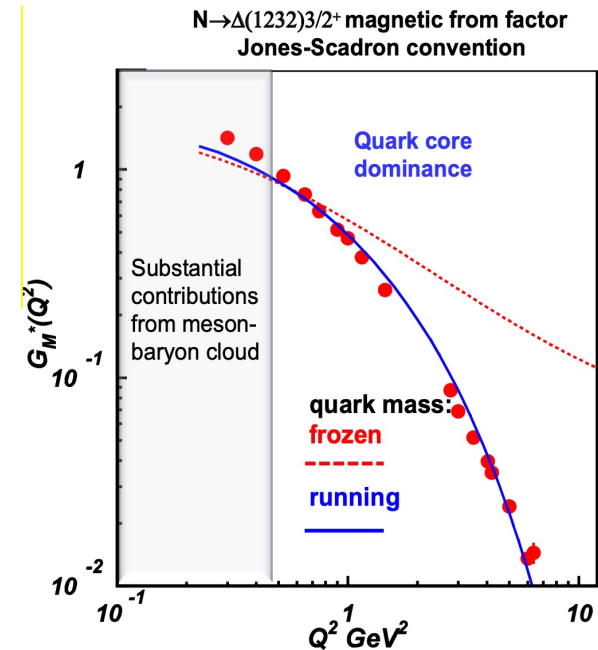
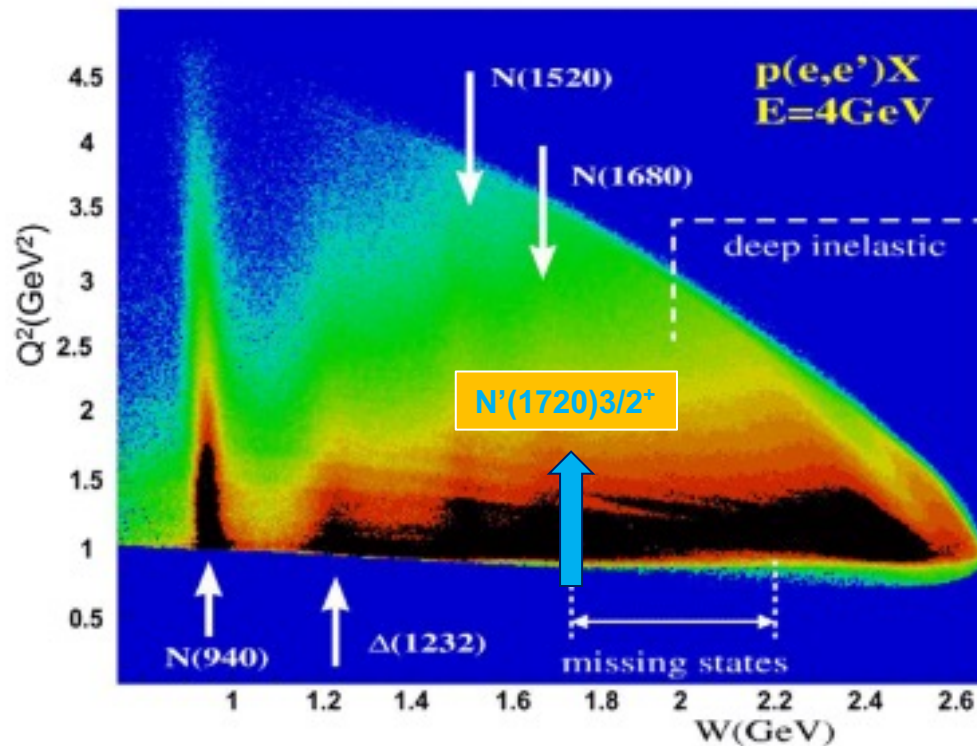


Photo- and Electrocouplings of Nucleon Resonances



V.I. Mokeev
Jefferson Laboratory
(CLAS Collaboration)



The 2021 School on the Physics of Baryons



Outline

- Motivation for the studies of the N^* spectrum and structure
- Facilities for N^* studies
- N^* spectrum and photocouplings from exclusive photoproduction data
- Discovery of “missing” resonances
- Extraction of $N \rightarrow N^*$ electroexcitation amplitudes
- Insight into emergence of hadron mass (EHM)
- New prospects for N^* spectrum studies in the exploration of combined exclusive meson photo-/electroproduction data
- New opportunities to explore EHM from the CLAS12 exclusive electroproduction data
- Hybrid baryons with CLAS12
- Towards the ultimate QCD facility

How the Ground/Excited Nucleon Masses Emerge?

Composition of the Nucleon Mass:

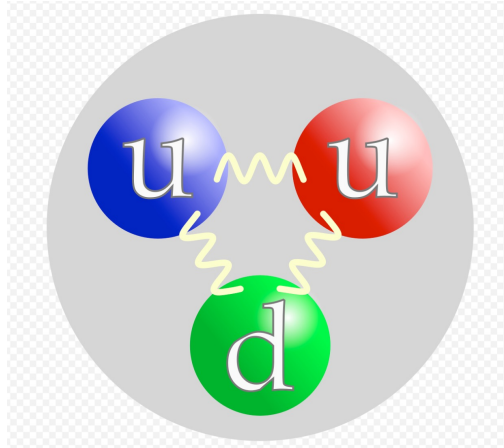
M_p , MeV (PDG20)

938.2720813
 ± 0.0000058

Sum of bare quark
masses, MeV

$2.16 + 2.16 + 4.67$
 $= 8.99^{+1.45}_{-0.65}$ or $< 1.1\%$

proton



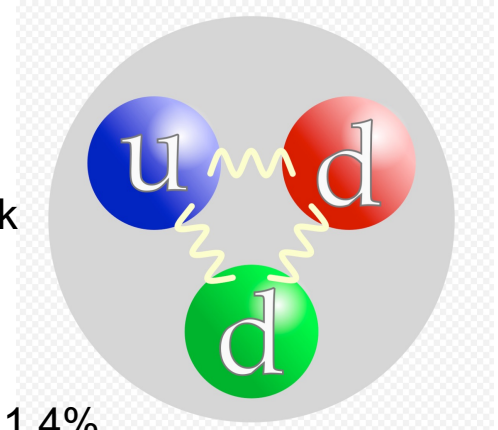
M_n , MeV (PDG20)

939.5654133
 ± 0.0000058

Sum of bare quark
masses, MeV

$4.67 + 4.67 + 2.16$
 $= 11.50^{+1.45}_{-0.60}$ or $< 1.4\%$

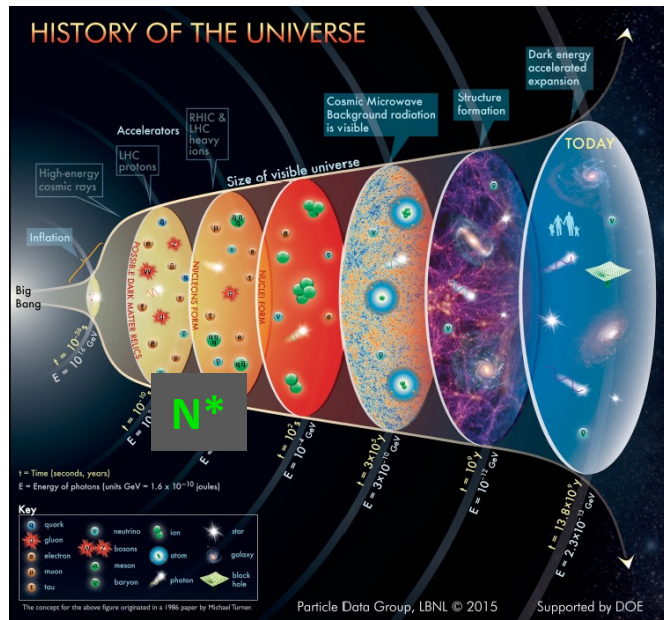
neutron



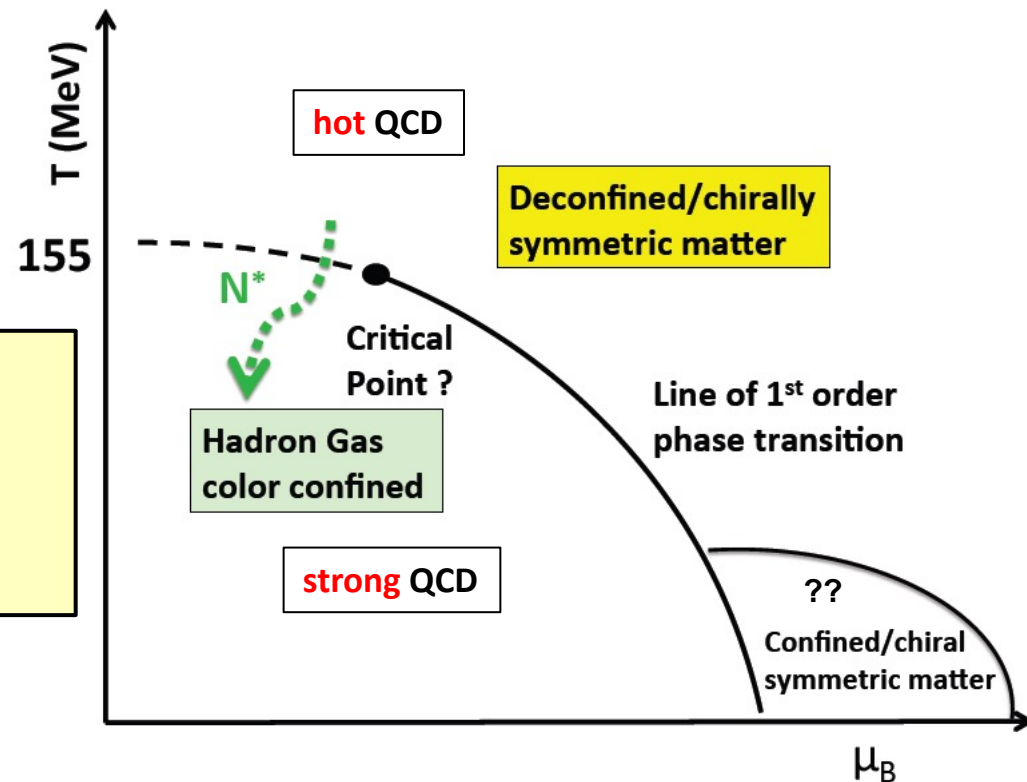
- Higgs mechanism generates the masses of bare quarks.
- Dominant part of nucleon mass is generated in processes other than the Higgs mechanism.

Studies of nucleon resonance electroexcitation within a broad range of photon virtuality Q^2 shed light on emergence of the dominant part of hadron mass in the transition from perturbative to quark-gluon confinement regimes of strong interaction.

Role of Nucleon Resonances in the Emergence of Hadronic Matter



Dramatic events occurred in the micro-second old universe during the transition from the deconfined quark and gluon phase to the hadron phase.



- Quark-gluon confinement emerges
- Chiral symmetry of QCD is broken
- Quarks and gluons acquire mass
- Baryon resonances form

This transition was shaped by the full meson and baryon spectra

Nobel Prize Achievements in the Ground and Excited Nucleon Exploration



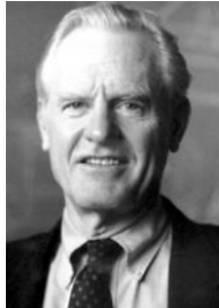
1961

"for his pioneering studies of electron scattering in atomic nuclei and for his thereby achieved discoveries concerning the structure of the nucleons"

R. Hofstadter



J.I. Friedman



H.W. Kendall



R.E. Taylor

1990

"for their pioneering investigations concerning deep inelastic scattering of electrons on protons and bound neutrons, which have been of essential importance for the development of the quark model in particle physics".



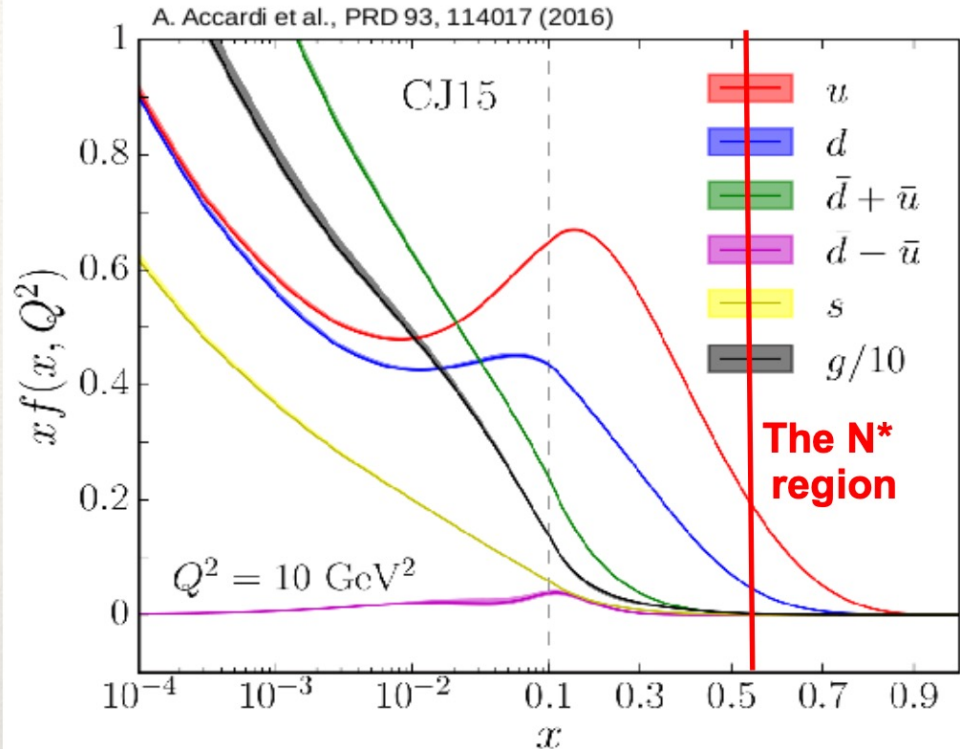
L.W. Alvarez

1968

"for his decisive contributions to elementary particle physics, in particular the discovery of a large number of resonance states, made possible through his development of the technique of using hydrogen bubble chamber and data analysis".

Revealing Ground Nucleon Constituents from DIS Studies

Nucleons and atomic nuclei account for most of the visible mass in the Universe



Particular features of nucleon structure:

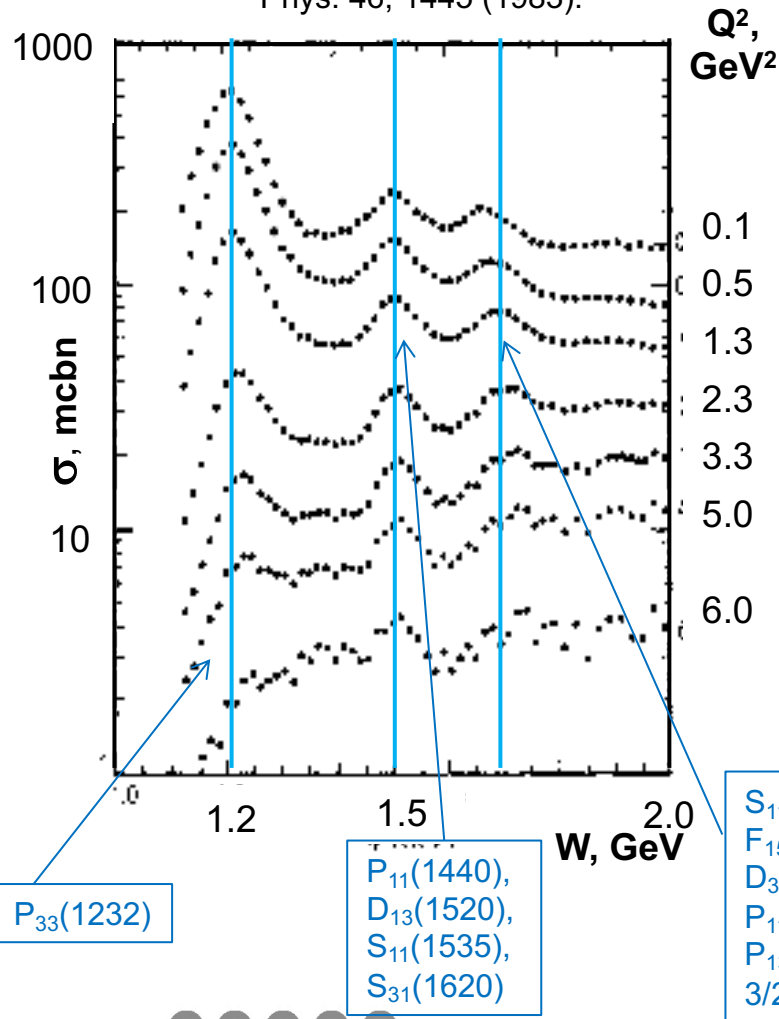
- the current quarks and gauge gluons are in permanent creation/annihilation processes;
- relativistic objects moving with velocities comparable with the velocity of light;
- quarks and gluons are always confined inside the hadrons; they are never free.

Such a complex composite system should possess a rich spectrum of excited states.

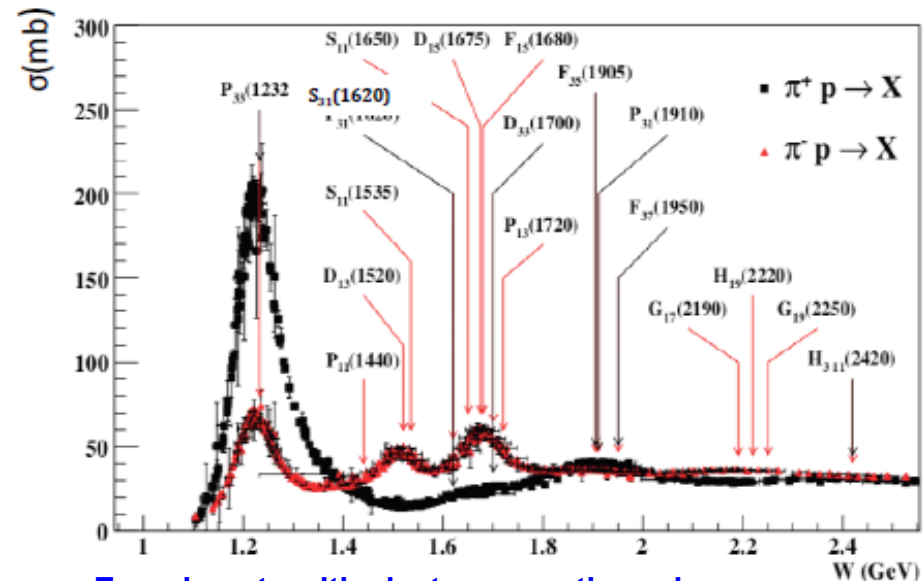
Nucleon Resonances (N*) in Inclusive Processes with Electron and Hadron Beams

Nucleon resonances in total virtual photon cross section

F. Foster and G. Hughes, Rep. Prog. Phys. 46, 1445 (1983).

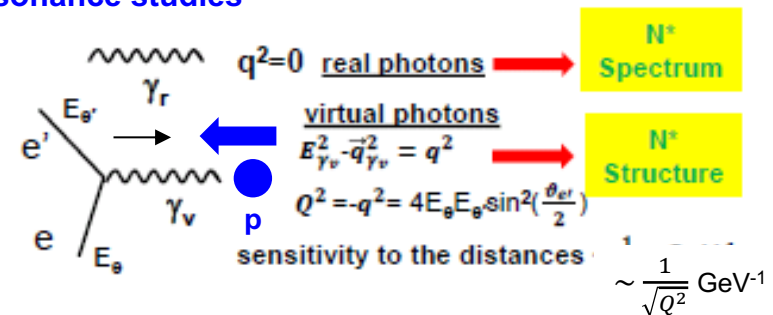


Nucleon resonances from hadroproduction data



Experiments with electromagnetic probes are:

- the only source of information on the structure of excited nucleon states;
- promising tool for new baryon state search and high-lying resonance studies



$W=M_{N^*}$ map-out N^* structure by varying Q^2

Resonant Structure Impact on Inclusive $F_2(W, Q^2)$ Structure Functions

Data points are from interpolation of the CLAS results re-evaluated with the σ_L/σ_T ratio from Hall C data

CLAS data:

M. Osipenko et al., PRD 67, 092001 (2003)

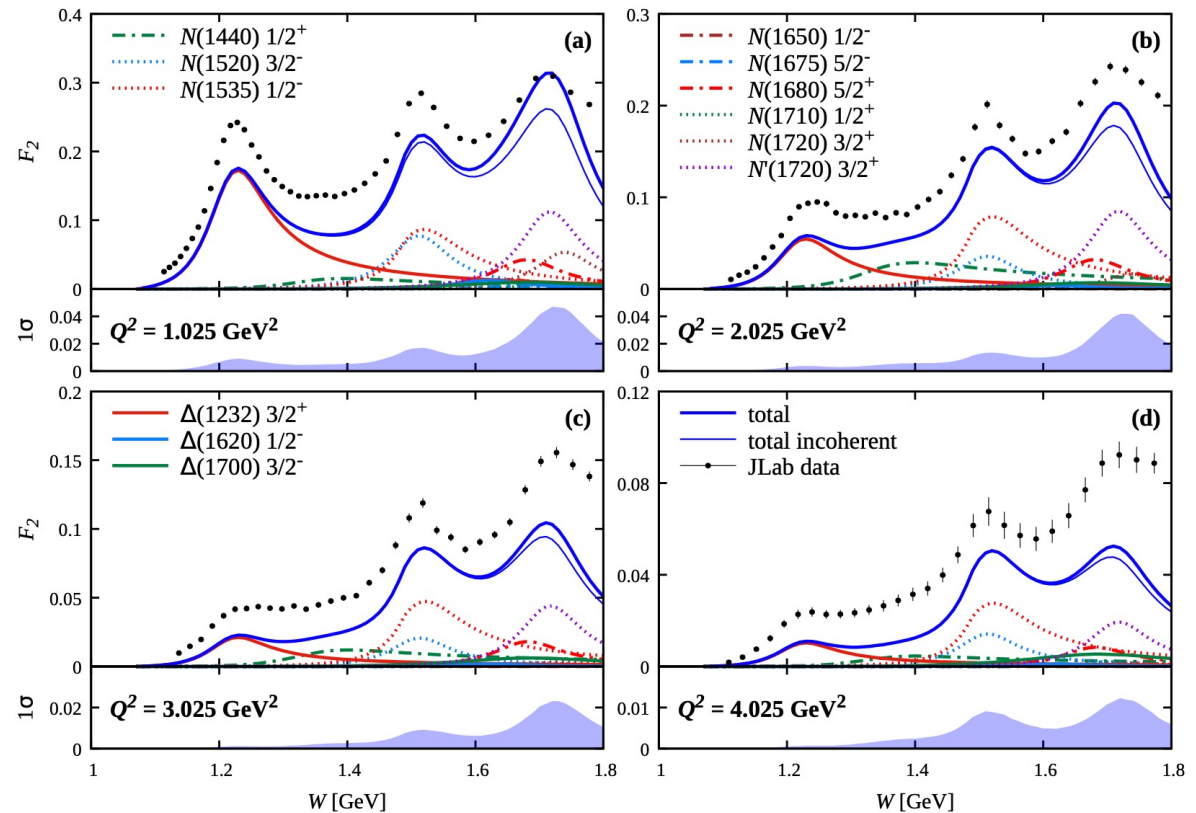
Hall C data:

Y. Liang, Ph.D., American Univ. (2003)

N^* contributions computed with $\gamma_p N^*$ electrocouplings from CLAS data:

A.N. Hiller Blin et al, PRC100, 035201 (2019);

A.N. Hiller Blin et al, PRC104, 025201 (2021)



- Differences in the structure of resonances contributing into three resonance-like maxima result in their different evolution with Q^2 .
- Studies of exclusive meson photo-/electroproduction are of particular importance to disentangle the contributions from different resonances and to explore the N^* spectrum and structure.

Facilities for N* studies from Exclusive Meson Photo- and Electroproduction Data

Measurements of exclusive meson photo-/electroproduction with continuous electron beam ($\sim 100\%$ duty factor) and with detectors of $\sim 4\pi$ acceptance are of particular importance for gaining insight into the N* spectrum and structure.

Exclusive photoproduction

D.G. Ireland et al, Prog. Nucl. Part Phys. 111, 103752 (2020)

Facility	W-coverage, GeV	Beam type/Flux	Country
CLAS/ JLab	1.1-3.0	Tagged bremsstrahlung, $10^8 \gamma/s$	USA
CLAS12/ JLab	1.1-4.0	Quasi-real photons, $L=10^{35} \text{ cm}^{-2}\text{s}^{-1}$	USA
GRAAL	1.1-1.9	Compton scattering, $10^6 \gamma/s$	France
MAMI	1.1-1.9	Tagged bremsstrahlung, $10^7 \gamma/s$	Germany
ELSA	1.1-2.7	Tagged bremsstrahlung, $10^7 \gamma/s$	Germany
Spring-8	1.1-2.5	Compton scattering, $10^6 \gamma/s$	Japan

Exclusive electroproduction

I.G. Aznauryan and V.D. Burkert, Progr. Nucl. Part. Phys. 67, 1 (2012)

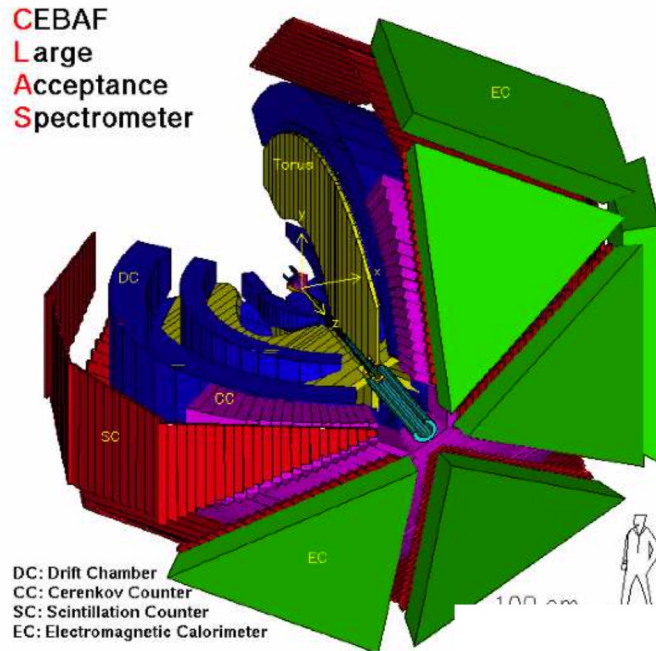
Facility	Q ² -coverage, GeV ²	W-coverage, GeV	Luminosity, cm ⁻² s ⁻¹	Country
CLAS/ JLab	0.2-5.0	1.1-2.5	10^{34}	USA
CLAS12/ JLab	0.05-10.0	1.1-4.0	10^{35}	USA
Halls A/C JLab	<7.0	1.1-1.8	10^{37}	USA
MAMI	<0.2	1.1-1.3	10^{36}	Germany
MIT Bates	<0.15	~ 1.23	10^{36}	USA

In red: decommissioned detectors

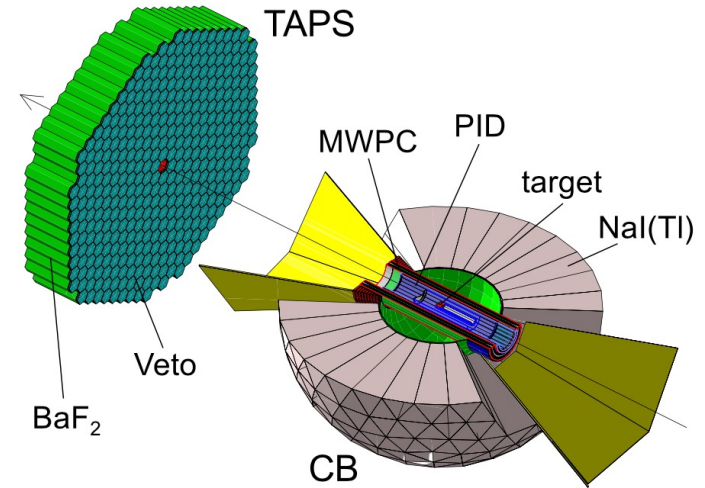
In magenta: spectrometers of small (msterad) acceptance



Detectors of Nearly 4π Acceptance for Studies of Exclusive Meson Photo- and Electroproduction



Momentum resolution for charged particles: 0.5-1.0%
 for γ/e^- : $\sigma/E = 10.3\% / \sqrt{E}$, GeV
 Polar angle resolution: < 1 mrad
 Azimuthal angle resolution: ~ 4 mrad
 Solid angle coverage for charged particles: $60\% \cdot 4\pi$



Resolution for electromagnetic showers in CB:
 $\Delta E/E = 0.02 / (E/\text{GeV})^{0.36}$.
 $\sigma_\theta \sim 2 - 3^\circ$
 $\sigma_\phi \sim 2^\circ / \sin \theta$.
 Solid angle coverage for charged particles: $97\% \cdot 4\pi$

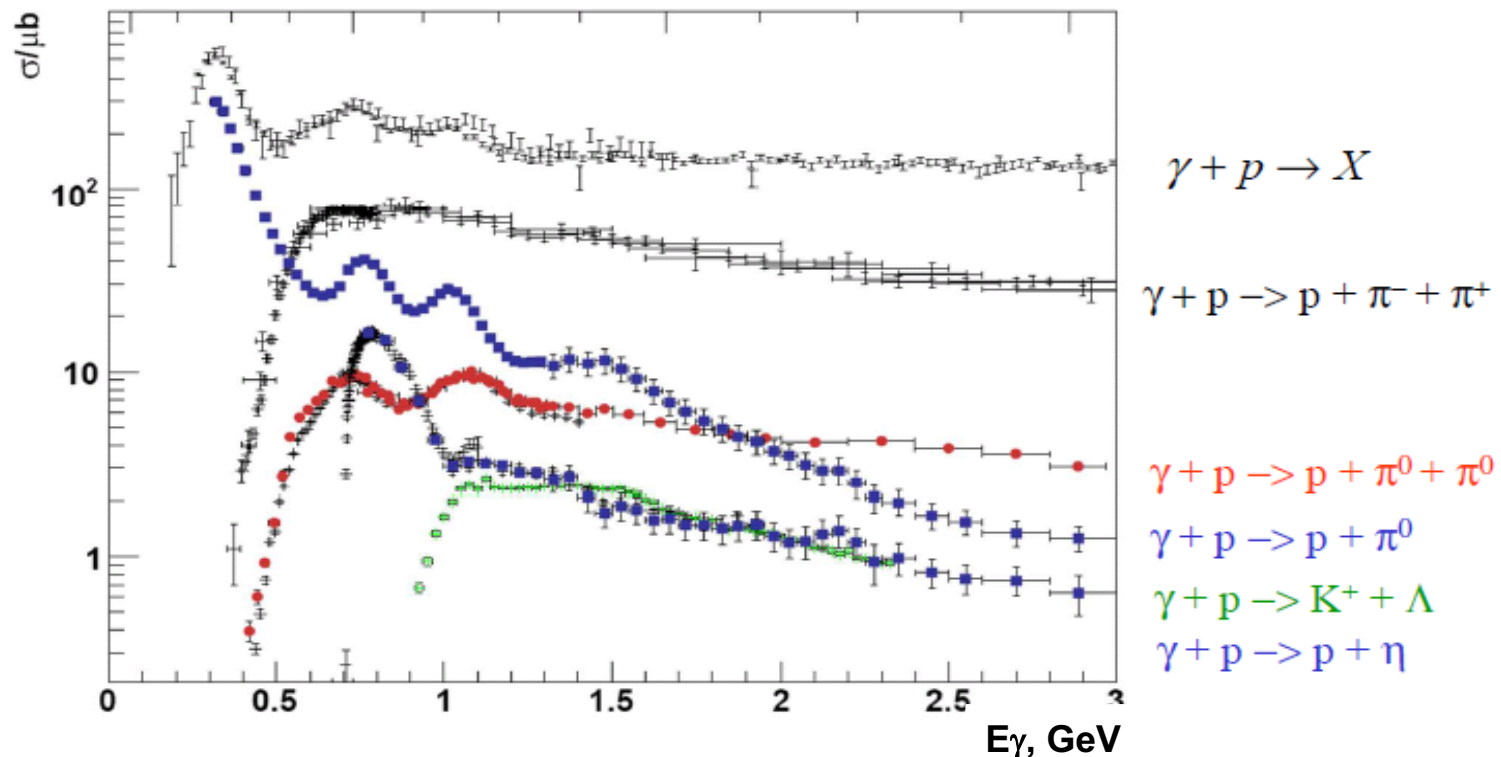
CLAS is the most suitable for the studies of exclusive charged meson photo-/electroproduction, while CB-TAPS is optimized for exploration of neutral meson photoproduction through their 2γ -decays

Exclusive Photoproduction in the Nucleon Resonance Region

Common effort at [ELSA, JLab](#) and [MAMI](#), [Spring-8](#)

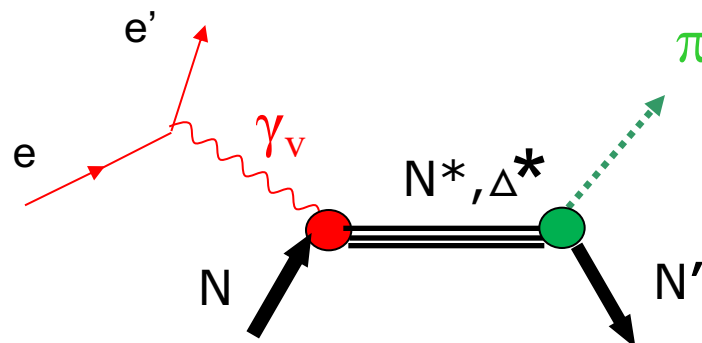
Combination of continuous electron beams and detectors of $\sim 4\pi$ acceptance allow us to determine types of all final state particles and their 4-momenta in each reaction.

Most exclusive photoproduction channels in the resonance region were studied.

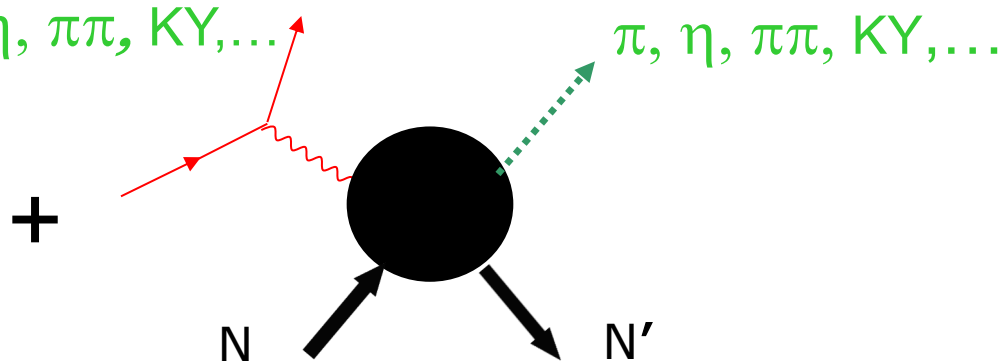


N* Photo-/Electroexcitation Amplitudes ($\gamma_{r,v}pN^*$ Photo-/Electrocouplings) and their Extraction from Exclusive Photo-/Electroproduction Data

Resonant amplitudes



Non-resonant amplitudes



- Real $A_{1/2}(Q^2)$, $A_{3/2}(Q^2)$, $S_{1/2}(Q^2)$

**I.G. Aznauryan and V.D. Burkert,
Prog. Part. Nucl. Phys. 67, 1 (2012)**

**Definition of N* photo-/electrocouplings
employed in CLAS data analyses:**

$$\Gamma_\gamma = \frac{k_{\gamma_{N^*}}^2}{\pi} \frac{2M_N}{(2J_r + 1)M_{N^*}} \left[|A_{1/2}|^2 + |A_{3/2}|^2 \right]$$

- N* parameters can be determined either within reaction models by fitting them to the data or inferred from the reaction amplitude singularities at the second Riemann sheet after their analytical continuation into the complex energy plane.
- Consistent results on $\gamma_{r,v}pN^*$ photo-/electrocouplings from different meson photo-/electro-production channels allow us to validate reliable extraction of these quantities.


Available vs. Needed Observables to Determine the Pseudoscalar Meson-Baryon Photoproduction Amplitudes

$\gamma p \rightarrow MB$ reaction amplitude with mesons of zero spin and baryons of $\frac{1}{2}$ spin (πN , ηN , $K\Lambda$, $K\Sigma$ photoproduction):
 $\langle M\lambda_B | T(s,t) | \lambda_\gamma \lambda_p \rangle$ $\lambda_\gamma = +1, -1$; $\lambda_p = +1/2, -1/2$; $\lambda_B = +1/2, -1/2$ $\rightarrow 2 \times 2 \times 2 = 8$ amplitudes \rightarrow Parity conservation
 $\rightarrow 4$ independent amplitudes or 8 real numbers \rightarrow Invariance under phase rotation \rightarrow
 7 real numbers.

At least seven independent observables are needed in each bin of (s,t) to reconstruct the pseudoscalar meson-baryon photoproduction amplitudes

filled boxes: data acquired

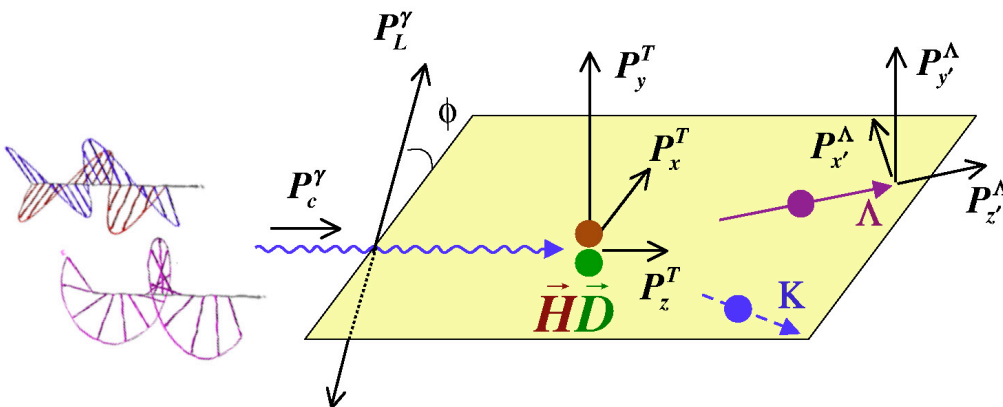
✓ - analyzed/published

Observable	σ	Σ	T	P	E	F	G	H	T_x	T_z	L_x	L_z	O_x	O_z	C_x	C_z		
$p\pi^0$	✓	✓	✓		✓	✓	✓	✓										
$n\pi^+$	✓	✓	✓		✓	✓	✓	✓	<div><div>$\gamma p \rightarrow X$</div><div></div></div>									
$p\eta$	✓	✓	✓		✓	✓	✓	✓										
$p\eta'$	✓	✓	✓		✓	✓	✓	✓										
$K^+\Lambda$	✓	✓	✓	✓	✓	✓	✓	✓									✓	✓
$K^+\Sigma^0$	✓	✓	✓	✓	✓	✓	✓	✓	✓	✓	✓	✓	✓	✓	✓	✓		
$K^{*+}\Lambda$	✓			✓					SDME									
$K^{*0}\Sigma^+$	✓	✓									✓	✓	SDME					

Observables from the Meson-Baryon Photoproduction Channels

[SHKL, J Phys G38 (11) 053001]

Photon beam		Target			Recoil			Target - Recoil								
					x'	y'	z'	x'	x'	x'	y'	y'	y'	z'	z'	z'
		x	y	z				x	y	z	x	y	z	x	y	z
unpolarized	σ_0		T			P		$T_{x'}$		$L_{x'}$		Σ		$T_{z'}$		$L_{z'}$
$P_L^\gamma \sin(2\phi_\gamma)$		H		G	$O_{x'}$		$O_{z'}$		$C_{z'}$		E		F		$-C_{x'}$	
$P_L^\gamma \cos(2\phi_\gamma)$	$-\Sigma$		$-P$			$-T$		$-L_{z'}$		$T_{z'}$		$-\sigma_0$		$L_{x'}$		$-T_{x'}$
circular P_c^γ		F		$-E$	$C_{x'}$		$C_{z'}$		$-O_{z'}$		G		$-H$		$O_{x'}$	



16 different observables

- They are described by different bilinear combinations of amplitudes
- Combined fit of all observables offers rigorous constraints on the reaction amplitude at the real energy axis

Extraction of Differential Cross Sections and Polarization Observables

$$\mathbf{d}\sigma^{\mathbf{B},\mathbf{T},\mathbf{R}}(\vec{P}^\gamma, \vec{P}^T, \vec{P}^R, \phi) = \frac{1}{2} \left\{ \mathbf{d}\sigma_0 \left[1 - P_L^\gamma P_y^T P_{y'}^R \cos 2(\alpha - \phi) \right] \right. \quad (1a)$$

$$\text{Single spin observables} \quad + \mathbf{\Sigma} \left[-P_L^\gamma \cos 2(\alpha - \phi) + P_y^T P_{y'}^R \right] \quad (1b)$$

$$+ \mathbf{T} \left[P_y^T - P_L^\gamma P_{y'}^R \cos 2(\alpha - \phi) \right] \quad (1c)$$

$$+ \mathbf{P} \left[P_{y'}^R - P_L^\gamma P_y^T \cos 2(\alpha - \phi) \right] \quad (1d)$$

$$\text{Beam-Target observables} \quad + \mathbf{E} \left[-P_\odot^\gamma P_z^T + P_L^\gamma P_x^T P_{y'}^R \sin 2(\alpha - \phi) \right] \quad (1e)$$

$$+ \mathbf{G} \left[P_L^\gamma P_z^T \sin 2(\alpha - \phi) + P_\odot^\gamma P_x^T P_{y'}^R \right] \quad (1f)$$

$$+ \mathbf{F} \left[P_\odot^\gamma P_x^T + P_L^\gamma P_z^T P_{y'}^R \sin 2(\alpha - \phi) \right] \quad (1g)$$

$$+ \mathbf{H} \left[P_L^\gamma P_x^T \sin 2(\alpha - \phi) - P_\odot^\gamma P_x^T P_{y'}^R \right] \quad (1h)$$

$$\text{Beam-Recoil observables} \quad + \mathbf{C}_{\mathbf{x}'} \left[P_\odot^\gamma P_{x'}^R - P_L^\gamma P_y^T P_{z'}^R \sin 2(\alpha - \phi) \right] \quad (1i)$$

$$+ \mathbf{C}_{\mathbf{z}'} \left[P_\odot^\gamma P_{z'}^R - P_L^\gamma P_y^T P_{x'}^R \sin 2(\alpha - \phi) \right] \quad (1j)$$

$$+ \mathbf{O}_{\mathbf{x}'} \left[P_L^\gamma P_{x'}^R \sin 2(\alpha - \phi) + P_\odot^\gamma P_y^T P_{z'}^R \right] \quad (1k)$$

$$+ \mathbf{O}_{\mathbf{z}'} \left[P_L^\gamma P_{z'}^R \sin 2(\alpha - \phi) - P_\odot^\gamma P_y^T P_{x'}^R \right] \quad (1l)$$

$$\text{Target-Recoil observables} \quad + \mathbf{L}_{\mathbf{x}'} \left[P_z^T P_{x'}^R + P_L^\gamma P_x^T P_{z'}^R \cos 2(\alpha - \phi) \right] \quad (1m)$$

$$+ \mathbf{L}_{\mathbf{z}'} \left[P_z^T P_{z'}^R - P_L^\gamma P_x^T P_{x'}^R \cos 2(\alpha - \phi) \right] \quad (1n)$$

$$+ \mathbf{T}_{\mathbf{x}'} \left[P_x^T P_{x'}^R + P_L^\gamma P_z^T P_{z'}^R \cos 2(\alpha - \phi) \right] \quad (1o)$$

$$+ \mathbf{T}_{\mathbf{z}'} \left[P_x^T P_{z'}^R - P_L^\gamma P_z^T P_{x'}^R \cos 2(\alpha - \phi) \right] \} \quad (1p)$$

D.G. Ireland et al, Prog. Nucl.
Part Phys. 111, 103752 (2020)



Connection between Pseudoscalar Meson-Baryon Photoproduction Observables and CGLN Amplitudes

$$d\sigma_0 = +\Re \{ F_1^* F_1 + F_2^* F_2 + \sin^2 \theta (F_3^* F_3 + F_4^* F_4) / 2 + \sin^2 \theta (F_2^* F_3 + F_1^* F_4 + \cos \theta F_3^* F_4) - 2 \cos \theta F_1^* F_2 \} \rho_0, \quad (58a)$$

$$\hat{\Sigma} = -\sin^2 \theta \Re \{ (F_3^* F_3 + F_4^* F_4) / 2 + F_2^* F_3 + F_1^* F_4 + \cos \theta F_3^* F_4 \} \rho_0, \quad (58b)$$

$$\hat{T} = +\sin \theta \Im \{ F_1^* F_3 - F_2^* F_4 + \cos \theta (F_1^* F_4 - F_2^* F_3) - \sin^2 \theta F_3^* F_4 \} \rho_0, \quad (58c)$$

$$\hat{P} = -\sin \theta \Im \{ 2F_1^* F_2 + F_1^* F_3 - F_2^* F_4 - \cos \theta (F_2^* F_3 - F_1^* F_4) - \sin^2 \theta F_3^* F_4 \} \rho_0, \quad (58d)$$

$$\hat{E} = +\Re \{ F_1^* F_1 + F_2^* F_2 - 2 \cos \theta F_1^* F_2 + \sin^2 \theta (F_2^* F_3 + F_1^* F_4) \} \rho_0, \quad (58e)$$

$$\hat{G} = +\sin^2 \theta \Im \{ F_2^* F_3 + F_1^* F_4 \} \rho_0, \quad (58f)$$

$$\hat{F} = +\sin \theta \Re \{ F_1^* F_3 - F_2^* F_4 - \cos \theta (F_2^* F_3 - F_1^* F_4) \} \rho_0, \quad (58g)$$

$$\hat{H} = -\sin \theta \Im \{ 2F_1^* F_2 + F_1^* F_3 - F_2^* F_4 + \cos \theta (F_1^* F_4 - F_2^* F_3) \} \rho_0, \quad (58h)$$

$$\hat{C}_{x'} = -\sin \theta \Re \{ F_1^* F_1 - F_2^* F_2 - F_2^* F_3 + F_1^* F_4 - \cos \theta (F_2^* F_4 - F_1^* F_3) \} \rho_0, \quad (58i)$$

$$\hat{C}_{z'} = -\Re \{ 2F_1^* F_2 - \cos \theta (F_1^* F_1 + F_2^* F_2) + \sin^2 \theta (F_1^* F_3 + F_2^* F_4) \} \rho_0, \quad (58j)$$

$$\hat{O}_{x'} = -\sin \theta \Im \{ F_2^* F_3 - F_1^* F_4 + \cos \theta (F_2^* F_4 - F_1^* F_3) \} \rho_0, \quad (58k)$$

$$\hat{O}_{z'} = +\sin^2 \theta \Im \{ F_1^* F_3 + F_2^* F_4 \} \rho_0, \quad (58l)$$

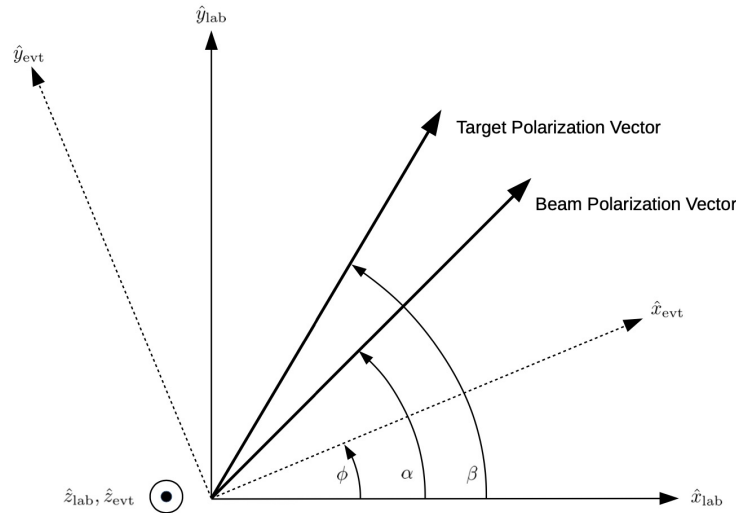
$$\hat{L}_{x'} = +\sin \theta \Re \{ F_1^* F_1 - F_2^* F_2 - F_2^* F_3 + F_1^* F_4 + \sin^2 \theta (F_4^* F_4 - F_3^* F_3) / 2 + \cos \theta (F_1^* F_3 - F_2^* F_4) \} \rho_0, \quad (58m)$$

$$\hat{L}_{z'} = +\Re \{ 2F_1^* F_2 - \cos \theta (F_1^* F_1 + F_2^* F_2) + \sin^2 \theta (F_1^* F_3 + F_2^* F_4 + F_3^* F_4) + \cos \theta \sin^2 \theta (F_3^* F_3 + F_4^* F_4) / 2 \} \rho_0, \quad (58n)$$

$$\hat{T}_{x'} = -\sin^2 \theta \Re \{ F_1^* F_3 + F_2^* F_4 + F_3^* F_4 + \cos \theta (F_3^* F_3 + F_4^* F_4) / 2 \} \rho_0, \quad (58o)$$

$$\hat{T}_{z'} = +\sin \theta \Re \{ F_1^* F_4 - F_2^* F_3 + \cos \theta (F_1^* F_3 - F_2^* F_4) + \sin^2 \theta (F_4^* F_4 - F_3^* F_3) / 2 \} \rho_0. \quad (58p)$$

From Observables in Meson-Baryon Photoproduction to Reaction Amplitudes



16 independent observables shown in red in slide #15 can be related to the bi-linear combinations of the meson-baryon photoproduction amplitudes as described in slide #16.
A.M. Sandorfi et al., J. Phys. G38, 053001 (2011)

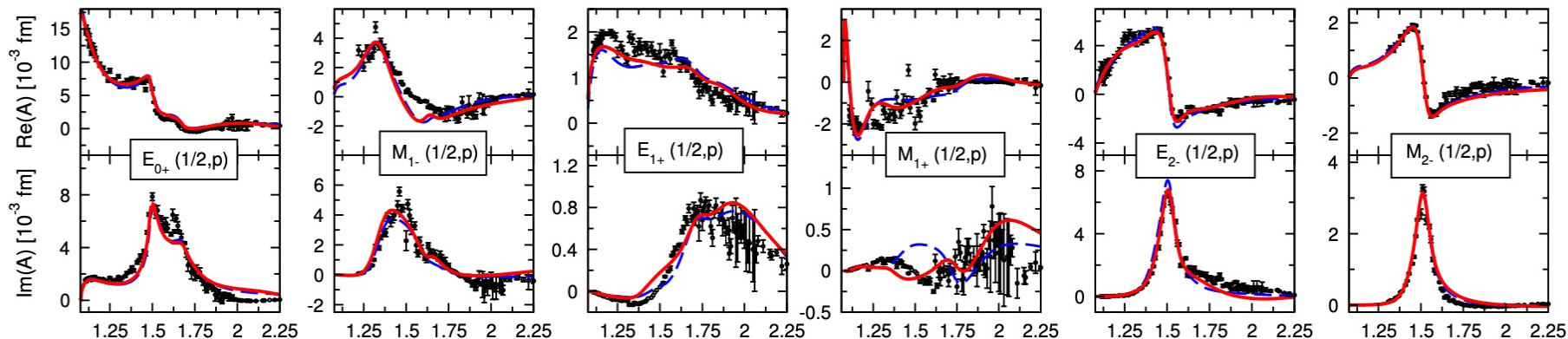
Figure 2: The definitions of laboratory and event axes, as well as azimuthal angles. The common laboratory, center-of-mass and event z -axis is directed out of the page. The lab x - and y -axes are in the horizontal and vertical directions, and the event y -axis is normal to the reaction plane.

- Seven observables are available for $N\pi$ channel and 16 for $K\Lambda$ and $K\Sigma$ channels offering an opportunity to gain insight into $N\pi$ and KY photoproduction amplitudes from the data.

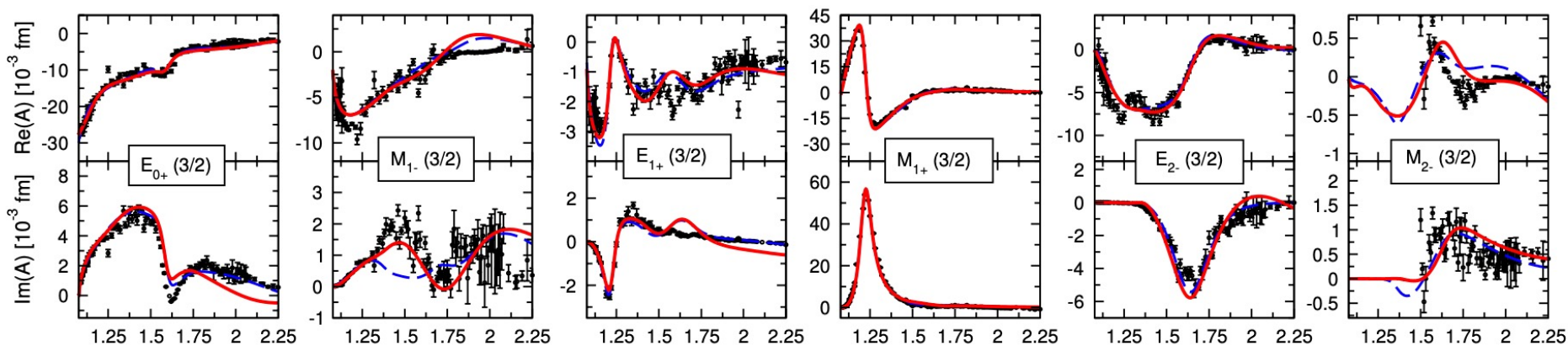
Problems: Limited coverage of the reaction phase space, data uncertainties, different parameterization of the reaction amplitudes to cover full reaction phase space, different amplitude appearance owing to invariance under common phase rotation.

$N\pi$ Photoproduction Amplitudes

$I=1/2$



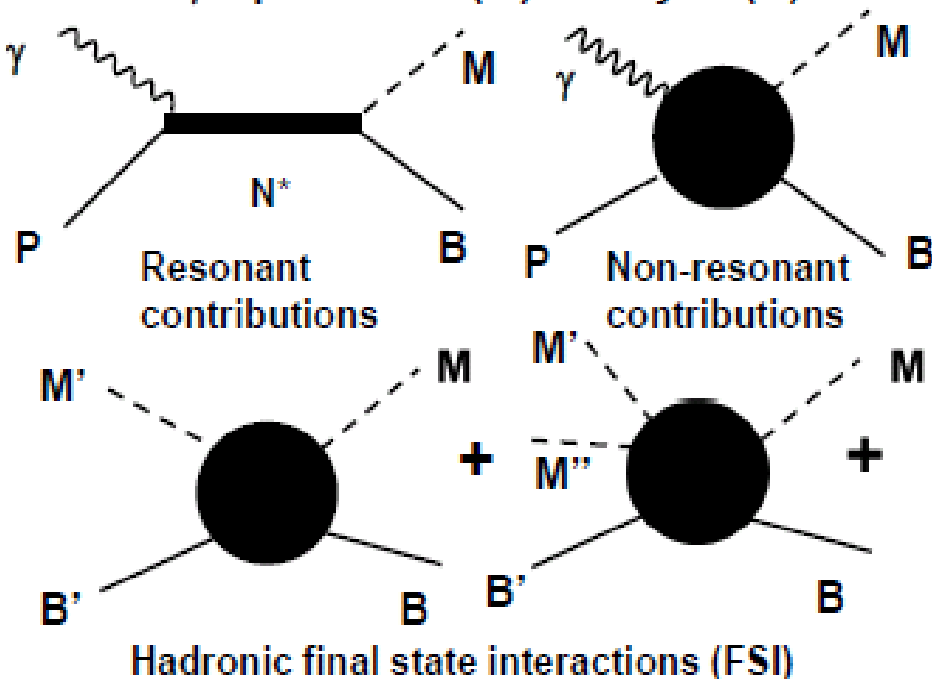
$I=3/2$



Multipoles extraction from the data (SAID): R.L. Workman et al., Phys. Rev. C86, 015202 (2012)

Multipoles from coupled channel approach: D. Ronchen et al., Eur. Phys. J. A50, 6 (2014)

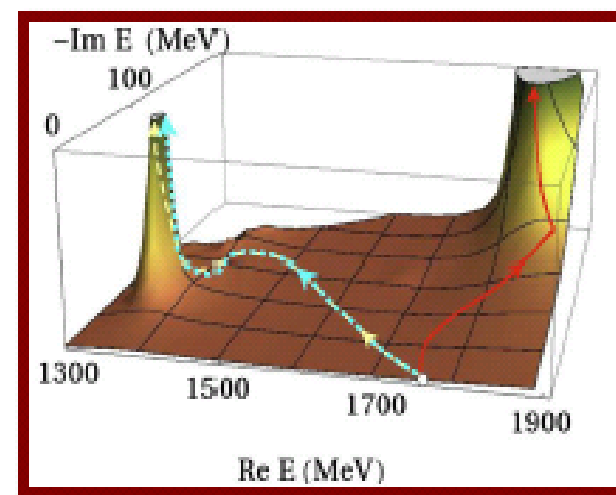
$\gamma + p \rightarrow \text{Meson (M)} + \text{Baryon (B)}$



See the upcoming talk by M. Doering on advanced global multi-channel analyses

Breit-Wigner parameterization and the amplitude poles:

$$T_{res} = \frac{R(M_{N^*}^2 - W^2) + Ri\Gamma_{N^*}(W)M_{N^*}}{(M_{N^*}^2 - W^2)^2 + (\Gamma_{N^*}(W)M_{N^*})^2}$$



- Constrain exclusive photoproduction amplitudes by fitting them to the differential cross sections and polarization asymmetries.
- Incorporate the FSI effects → Global multi-channel analyses of all exclusive photo-/hadro-production channels.
- Make analytical continuation of reaction amplitudes into the complex energy plane and:
 - a) locate poles → Resonance masses (M_{N^*}) and total widths (Γ_{N^*});
 - b) determine residues → Resonance photocouplings and partial hadronic decay widths.

Approaches for Extraction of the Nucleon Resonance Parameters from Exclusive Meson Photoproduction

Independent analyses of different exclusive channels:

SAID:

R. L. Workman et al, Phys. Rev C86, 015202 (2012)

R. L. Workman et al, Phys. Rev C95, 015206 (2017)

MAID:

D. Drechsel et al., Eur. Phys. J. A34, 69 (2007)

L. Tiator et al, Eur. Phys. J. A54, 210 (2018)

L. Tiator, Few Body Syst. 59, 21 (2018)

Global coupled channel analyses:

Bonn-Gatchina:

A. Anisovich et al., Eur. Phys. J. A48, 15 (2012)

A. Anisovich et al., Eur. Phys. J. A53, 242 (2017)

Argonne-Osaka:

H. Kamano et al., Phys. Rev. C94, 015201 (2016)

H. Kamano et al., Phys. Rev. C68, 035209 (2013)

Julich-Bonn-Washington:

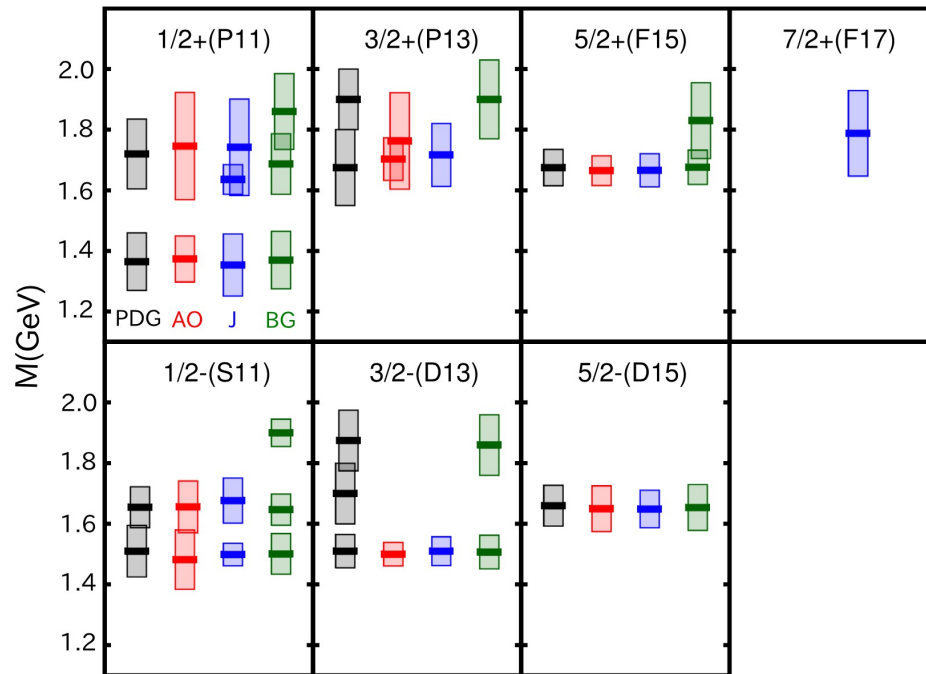
D. Roenchen et al., Eur. Phys. J. A50, 101 (2014)

J. Landay et al., Phys. Rev. D99, 016001 (2019)

Consistent results from independent analyses of different exclusive meson photoproduction channels and from the global multi-channel analyses are important to determine the uncertainties of the resonance parameters extracted from the data.

N* Spectrum from Global Multi-Channel Analyses of Photoproduction Before 2017

H. Kamano et al., Phys. Rev. C88, 035209 (2013)

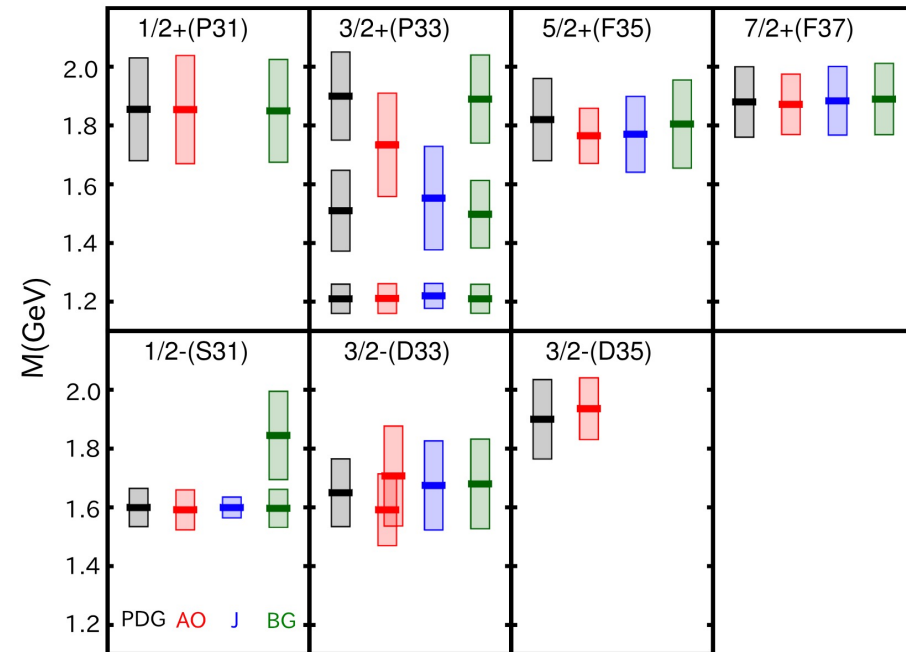


Analysis approaches:

AO: Argonne-Osaka

J: Julich-Bonn-Washington

BG: Bonn-Gatchina



Consistent results on the N* spectrum from different coupled-channel approaches in the mass range <1.6 GeV and evident difference for resonance masses, total decay widths, as well as in the number of excited states in the mass range above 1.6 GeV.

N* Photocouplings from Multi-Channel Analyses of Photoproduction Data

fit→	Re E_p	-2Im E_p	$A_{pole}^{1/2}$		$\vartheta^{1/2}$	
	[MeV]	[MeV]	[10 ⁻³ GeV ^{-1/2}]		[deg]	
	1	2	1	2	1	2
$N(1535) 1/2^-$	1498	74	57	50^{+4}_{-4}	-20	-14^{+12}_{-10}
BnGa [55]	1501 ± 4	134 ± 11		116 ± 10		7 ± 6
ANL-Osaka [68]	1482	196		161		9
SAID [246]	1502	95		77 ± 5		4
$N(1650) 1/2^-$	1677	146	27	23^{+3}_{-8}	21	6^{+28}_{-15}
BnGa [55]	1647 ± 6	103 ± 8		33 ± 7		-9 ± 15
ANL-Osaka [68]	1656	170		40		-44
SAID [246]	1648	80		35 ± 3		-16
$N(1440) 1/2^+_{(a)}$	1353	212	-58	-54^{+4}_{-3}	4	5^{+2}_{-5}
BnGa [55]	1370 ± 4	190 ± 7		-44 ± 7		-38 ± 5
ANL-Osaka [68]	1374	152		49		-10
SAID [246]	1359	162		-66 ± 5		-38
$N(1720) 3/2^+$	1717	208	39	51^{+5}_{-4}	96	57^{+9}_{-4}
BnGa [55]	1660 ± 30	450 ± 100		110 ± 45		0 ± 40
ANL-Osaka [68]	1703	140		234		2
$N(1520) 3/2^-$	1519	110	-27	-24^{+8}_{-3}	-11	-17^{+16}_{-6}
BnGa [55]	1507 ± 3	111 ± 5		-21 ± 4		0 ± 5
ANL-Osaka [68]	1501	78		38		2
SAID [246]	1515	113		-24 ± 3		-7
$N(1675) 5/2^-$	1650	126	22	22^{+4}_{-7}	36	49^{+5}_{-2}
BnGa [55]	1654 ± 4	151 ± 5		24 ± 3		-16 ± 5
ANL-Osaka [68]	1650	150		5		-22
$N(1680) 5/2^+$	1666	108	-12	-13^{+2}_{-5}	-28	-42^{+9}_{-18}
BnGa [55]	1676 ± 6	113 ± 4		-13 ± 4		-25 ± 22
ANL-Osaka [68]	1665	98		53		-5
$\Delta(1232) 3/2^+$	1220	86	-116	-114^{+10}_{-3}	-9	-9^{+4}_{-2}
BnGa [55]	1210 ± 1	99 ± 2		-131 ± 3.5		-19 ± 2
ANL-Osaka [68]	1211	102		-133		-15
SAID [246]	1211	99		-136 ± 5		-18

fit→	Re E_p	-2Im E_p	$A_{pole}^{1/2}$		$\vartheta^{1/2}$	
	[MeV]	[MeV]	[10 ⁻³ GeV ^{-1/2}]		[deg]	
	1	2	1	2	1	2
$\Delta(1620) 1/2^-$	1599	71	-28	-28^{+6}_{-2}	-173	-166^{+1}_{-4}
BnGa [55]	1597 ± 4	130 ± 9		52 ± 5		-9 ± 9
ANL-Osaka [68]	1592	136		113		-1

D. Ronchen et al., Eur. Phys. J. A50, 6 (2014)

$A_{pole}^{3/2}$ $\vartheta^{3/2}$

17	14^{+9}_{-3}	-177	102^{+29}_{-59}
	150 ± 35		65 ± 35
	70		173
114	117^{+6}_{-10}	27	26^{+2}_{-2}
	132 ± 9		2 ± 4
	94		-173
	157 ± 6		10
21	36^{+4}_{-5}	-60	-30^{+4}_{-4}
	26 ± 8		-19 ± 6
	33		-23
124	126^{+1}_{-2}	-8	-7^{+3}_{-2}
	134 ± 5		-2 ± 4
	38		-177
-231	-229^{+3}_{-4}	4	$3^{+0.3}_{-0.4}$
	-254 ± 4.5		-9 ± 1
	-257		-3
	-255 ± 5		-6



Photocouplings from Breit-Wigner Parameterization of the Resonant Amplitudes

$N(1535) \rightarrow p\gamma$, helicity-1/2 amplitude $A_{1/2}$

VALUE (GeV ^{-1/2})	DOCUMENT ID	TECN	COMMENT
0.090 to 0.120 (≈ 0.105) OUR ESTIMATE			
0.107 \pm 0.003	¹⁶ HUNT	19	DPWA Multichannel
0.101 \pm 0.007	SOKHOYAN	15A	DPWA Multichannel
0.091 \pm 0.004	¹⁶ SHKLYAR	13	DPWA Multichannel
0.128 \pm 0.004	¹⁶ WORKMAN	12A	DPWA $\gamma N \rightarrow N\pi$
0.091 \pm 0.002	¹⁶ DUGGER	07	DPWA $\gamma N \rightarrow \pi N$

$N(1440) \rightarrow p\gamma$, helicity-1/2 amplitude $A_{1/2}$

VALUE (GeV ^{-1/2})	DOCUMENT ID	TECN	COMMENT
-0.080 to -0.050 (≈ -0.065) OUR ESTIMATE			
-0.091 \pm 0.007	¹ HUNT	19	DPWA Multichannel
-0.061 \pm 0.006	SOKHOYAN	15A	DPWA Multichannel
-0.085 \pm 0.003	¹ SHKLYAR	13	DPWA Multichannel
-0.056 \pm 0.001	¹ WORKMAN	12A	DPWA $\gamma N \rightarrow N\pi$
-0.051 \pm 0.002	¹ DUGGER	07	DPWA $\gamma N \rightarrow \pi N$

$N(1520) \rightarrow p\gamma$, helicity-1/2 amplitude $A_{1/2}$

VALUE (GeV ^{-1/2})	DOCUMENT ID	TECN	COMMENT
-0.030 to -0.015 (≈ -0.025) OUR ESTIMATE			
-0.034 \pm 0.003	¹ HUNT	19	DPWA Multichannel
-0.024 \pm 0.004	SOKHOYAN	15A	DPWA Multichannel
-0.015 \pm 0.001	¹ SHKLYAR	13	DPWA Multichannel
-0.019 \pm 0.002	¹ WORKMAN	12A	DPWA $\gamma N \rightarrow N\pi$
-0.028 \pm 0.002	¹ DUGGER	07	DPWA $\gamma N \rightarrow \pi N$
-0.038 \pm 0.003	¹ AHRENS	02	DPWA $\gamma N \rightarrow \pi N$

$\Delta(1232) \rightarrow N\gamma$, helicity-1/2 amplitude $A_{1/2}$

VALUE (GeV ^{-1/2})	DOCUMENT ID	TECN	COMMENT
-0.142 to -0.129 (≈ -0.135) OUR ESTIMATE			
-0.146 \pm 0.002	¹ HUNT	19	DPWA Multichannel
-0.131 \pm 0.004	ANISOVICH	12A	DPWA Multichannel
-0.139 \pm 0.002	¹ WORKMAN	12A	DPWA $\gamma N \rightarrow N\pi$
-0.139 \pm 0.004	¹ DUGGER	07	DPWA $\gamma N \rightarrow \pi N$
-0.137 \pm 0.005	AHRENS	04A	DPWA $\vec{\gamma}\vec{p} \rightarrow N\pi$
-0.1357 \pm 0.0013 \pm 0.0037	BLANPIED	01	LEGS $\gamma p \rightarrow p\gamma, p\pi^0, n\pi^+$
-0.131 \pm 0.001	¹ BECK	00	IPWA $\vec{\gamma}p \rightarrow p\pi^0, n\pi^+$
-0.140 \pm 0.005	KAMALOV	99	DPWA $\gamma N \rightarrow \pi N$
-0.1294 \pm 0.0013	HANSTEIN	98	IPWA $\gamma N \rightarrow \pi N$
-0.1278 \pm 0.0012	DAVIDSON	97	DPWA $\gamma N \rightarrow \pi N$

- Resonance photocouplings determined at the pole position show more spread in comparison with evaluations at the resonant point of $W = M_{N^*}$ by employing the BW parameterization for the resonant amplitudes.
- More efforts from experiment and phenomenology are needed to provide consistent results on resonance photocouplings at the pole position.
- The connection between resonance photocouplings at the pole position and at the resonant point remains an open problem.

$N(1520) \rightarrow p\gamma$, helicity-3/2 amplitude $A_{3/2}$

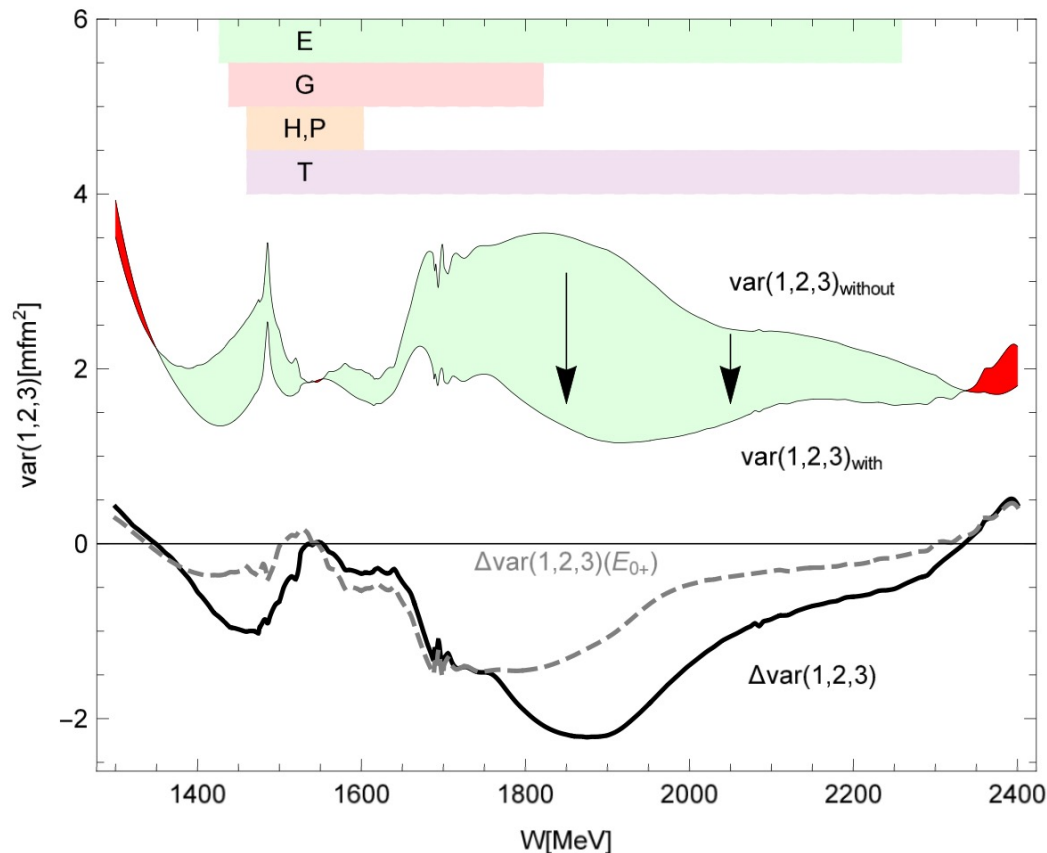
VALUE (GeV ^{-1/2})	DOCUMENT ID	TECN	COMMENT
0.135 to 0.145 (≈ 0.140) OUR ESTIMATE			
0.142 \pm 0.003	¹ HUNT	19	DPWA Multichannel
0.130 \pm 0.006	SOKHOYAN	15A	DPWA Multichannel
0.146 \pm 0.001	¹ SHKLYAR	13	DPWA Multichannel
0.141 \pm 0.002	¹ WORKMAN	12A	DPWA $\gamma N \rightarrow N\pi$
0.143 \pm 0.002	¹ DUGGER	07	DPWA $\gamma N \rightarrow \pi N$
0.147 \pm 0.010	¹ AHRENS	02	DPWA $\gamma N \rightarrow \pi N$

$\Delta(1232) \rightarrow N\gamma$, helicity-3/2 amplitude $A_{3/2}$

VALUE (GeV ^{-1/2})	DOCUMENT ID	TECN	COMMENT
-0.262 to -0.248 (≈ -0.255) OUR ESTIMATE			
-0.250 \pm 0.002	¹ HUNT	19	DPWA Multichannel
-0.254 \pm 0.005	ANISOVICH	12A	DPWA Multichannel
-0.262 \pm 0.003	WORKMAN	12A	DPWA $\gamma N \rightarrow N\pi$
-0.258 \pm 0.005	DUGGER	07	DPWA $\gamma N \rightarrow \pi N$
-0.256 \pm 0.003	AHRENS	04A	DPWA $\vec{\gamma}\vec{p} \rightarrow N\pi$
-0.2669 \pm 0.0016 \pm 0.0078	BLANPIED	01	LEGS $\gamma p \rightarrow p\gamma, p\pi^0, n\pi^+$
-0.251 \pm 0.001	BECK	00	IPWA $\vec{\gamma}p \rightarrow p\pi^0, n\pi^+$
-0.258 \pm 0.006	KAMALOV	99	DPWA $\gamma N \rightarrow \pi N$
-0.2466 \pm 0.0013	HANSTEIN	98	IPWA $\gamma N \rightarrow \pi N$
-0.2524 \pm 0.0013	DAVIDSON	97	DPWA $\gamma N \rightarrow \pi N$



Impact of the Experimental Data Extension on Convergency between $\pi^0 p$ Photoproduction Multipole from Different PWA Approaches



M. Doering, et al, PoS Hadron2017, 010 (2018)

Variances of $\pi^0 p$ photoproduction multipoles determined from SAID, Bonn-Gatchina, Jülich-Bonn-Washington PWA before/after implementation of the polarization observables. Top and bottom part show variances and their change, respectively. Variance is determined as the sum over squared difference in all multipoles up to $l=4$.

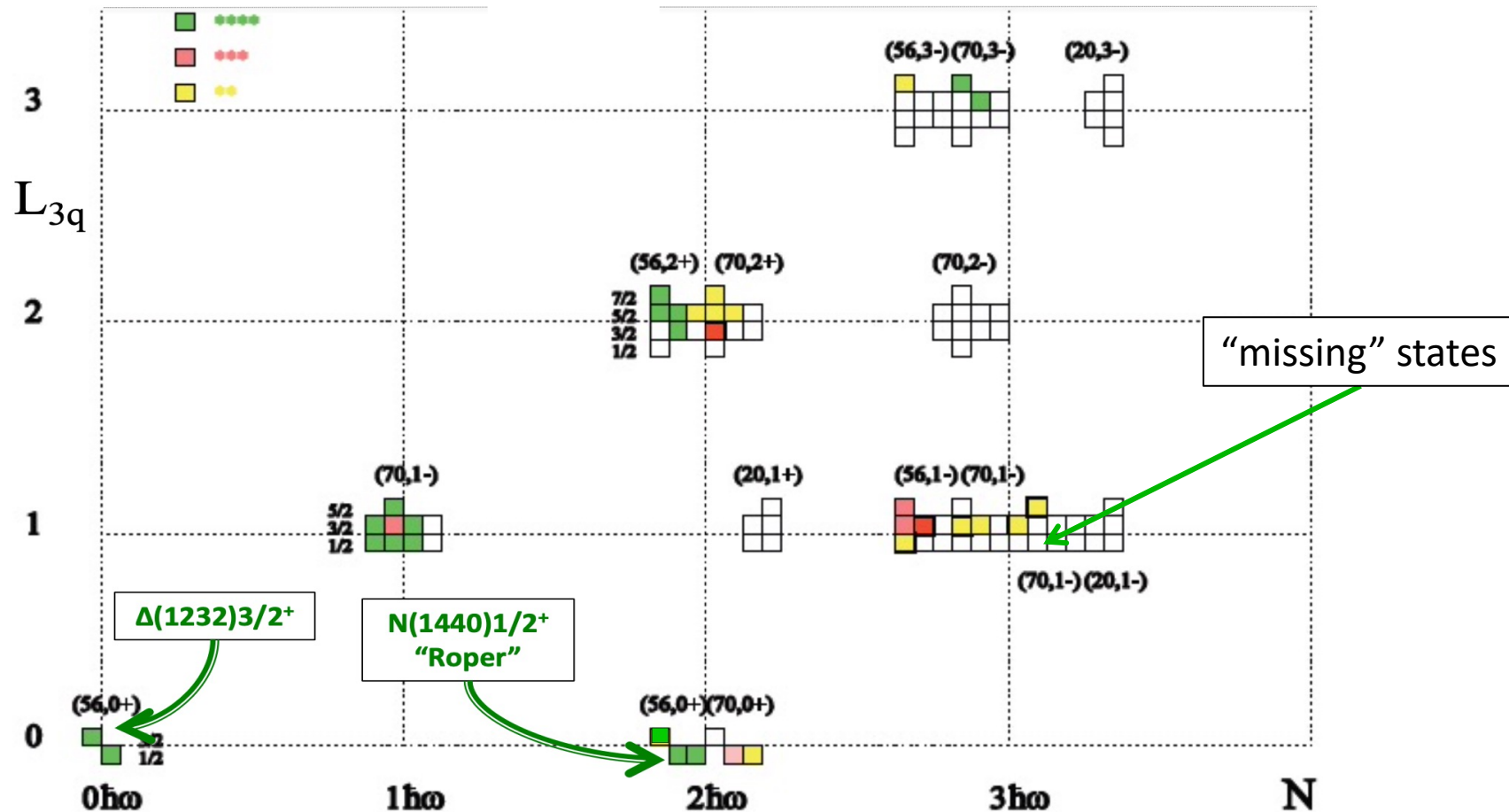
SU(6) \times O(3) Spin-Flavor Symmetry and ``Missing'' Resonances

PDG2012 status

Continuum QCD: C. Chen et al., PRD 100 (2019) 054009; Si-xue Qin et al., FBS 60 (2019) 26

Lattice QCD: R. Edwards et al., PRD 84 (2011) 074508

SU(6) \times O(3)



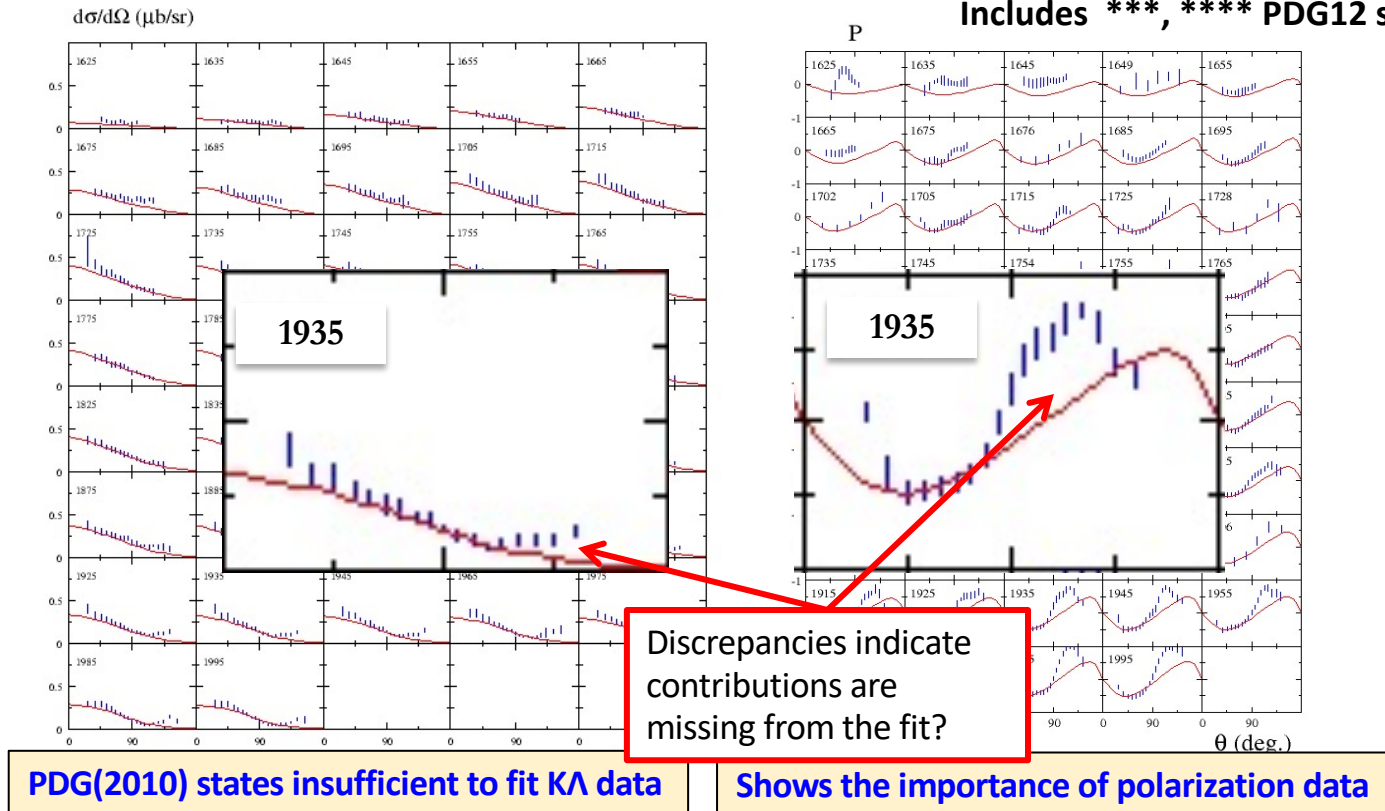
Studies of the N^* -spectrum were driven by a guess for the ``missing'' baryon states expected from underlying SU(6) \times O(3) symmetry and supported by continuum and lattice QCD results on the N^* -spectrum

Establishing the N^* Spectrum

Hyperon photoproduction $\gamma p \rightarrow K^+ \Lambda \rightarrow K^+ p \pi^-$ from CLAS

ANL-Osaka 8 coupled-channel analysis

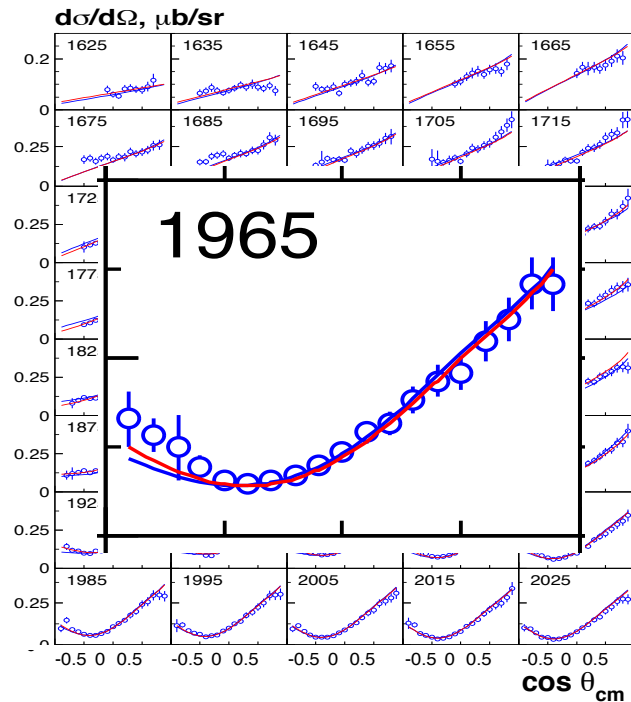
Includes ***, **** PDG12 states



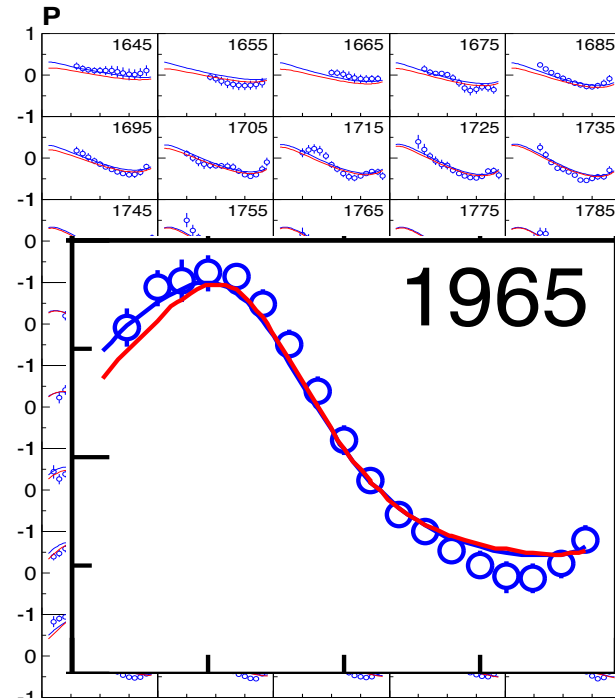
Establishing the N* Spectrum, cont'd

Hyperon photoproduction $\gamma p \rightarrow K^+ \Lambda \rightarrow K^+ p \pi^-$ from CLAS

Bonn-Gatchina multichannel analysis:
9 new resonances were included



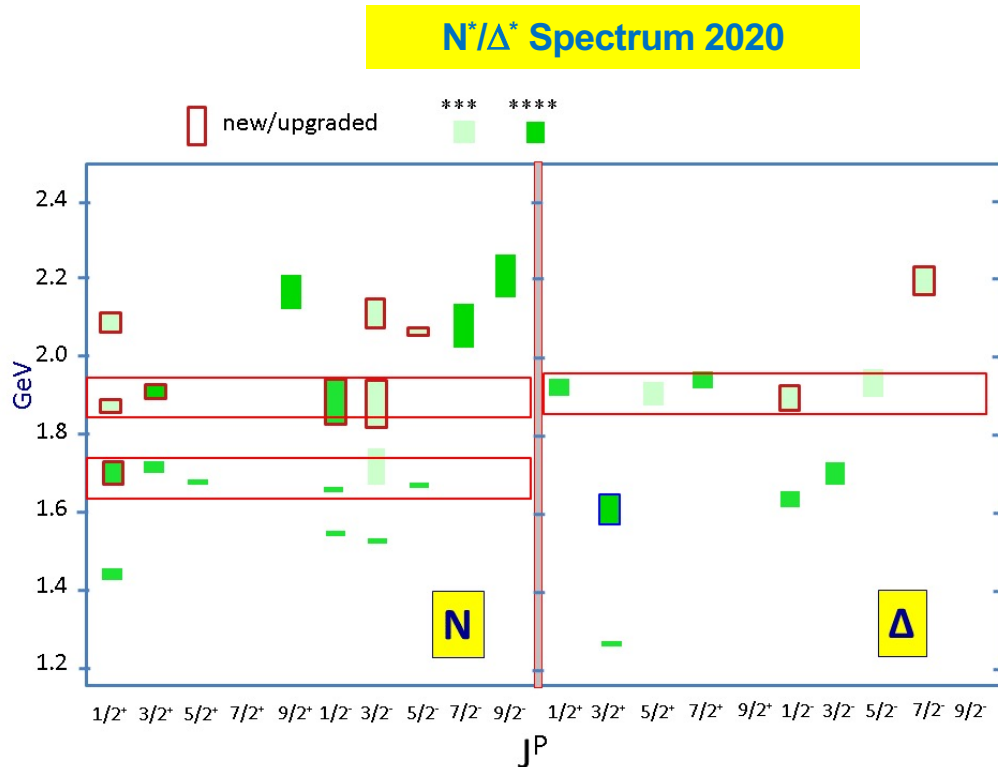
M. McCracken et al. (CLAS), Phys. Rev C 81, 025201 (2010)



A.V. Anisovich et al, EPJ A48, 15 (2012)

Advances in the Exploration of the N^* Spectrum in Photoproduction

Several **new nucleon resonances** were established in a global multi-channel analysis of exclusive photoproduction data



Nucleon resonances listed in Particle Data Group (PDG) tables

State $N(\text{mass})J^P$	PDG pre 2012	PDG 2020*
$N(1710)1/2^+$	***	****
$N(1880)1/2^+$		***
$N(1895)1/2^-$		****
$N(1900)3/2^+$	**	****
$N(1875)3/2^-$		***
$N(2100)1/2^+$	*	***
$N(2120)3/2^-$		***
$N(2000)5/2^+$	*	**
$N(2060)5/2^-$		***
$\Delta(1600)3/2^+$	***	****
$\Delta(1900)1/2^-$	**	***
$\Delta(2200)7/2^-$	*	***

Description of the exclusive electroproduction data off the proton with the same masses and hadronic decay widths as in photoproduction will validate the existence of new baryon states.

Combined studies of the CLAS $\pi^+\pi^-p$ photo-/electroproduction off proton data allow us to observe a new $N'(1720)3/2^+$ baryon state in addition to those listed above.

N* Structure in Experiments with CLAS/CLAS12

The experimental program on the studies of the N* structure in exclusive meson photo-/electroproduction with CLAS/CLAS12 seeks to determine:

- $\gamma_v p N^*$ electrocouplings at photon virtualities up to 10.0 GeV² for most of the excited proton states through analyzing major meson electroproduction channels from CLAS/CLAS12 data.
- Explore hadron mass emergence (EHM) and elucidating the trace anomaly by mapping out the dynamical quark mass in the transition from almost massless pQCD quarks to fully dressed constituent quarks.

An important part of the efforts on exploration of strong QCD from the data of the experiments with the electromagnetic probes:

1. S.J. Brodsky et al., Int. J. Mod. Phys. E29, 203006 (2020).
2. C.D. Roberts, Symmetry 12, 1468 (2020).
3. M. Barabanov et al., Prog. Part. Nucl. Phys. 103835 (2021).

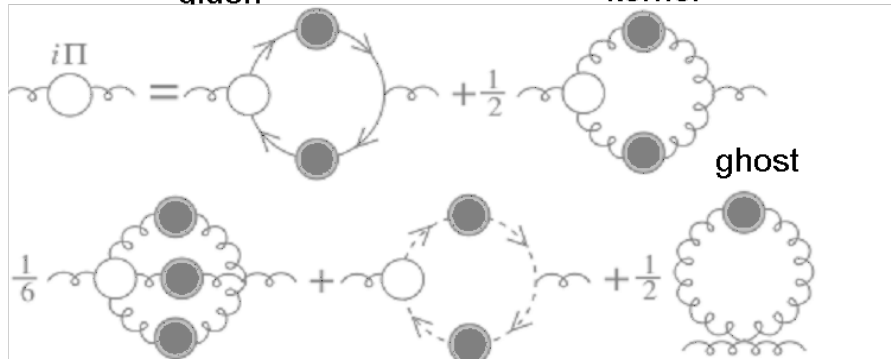
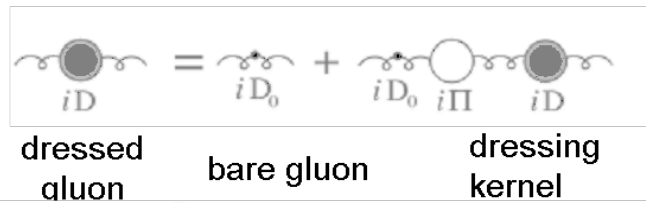
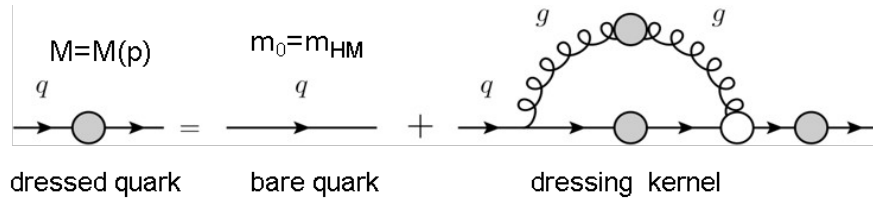
A unique source of information on many facets of strong QCD in generating excited nucleon states with different structural features:

1. I.G. Aznauryan and V.D. Burkert, Prog. Part. Nucl. Phys. 67, 1 (2012).
2. D.S. Carman, K. Joo, and V.I. Mokeev, Few Body Syst. 61, 29 (2020).
3. V.D. Burkert and C.D. Roberts, Rev. Mod. Phys. 91, 011003 (2019).

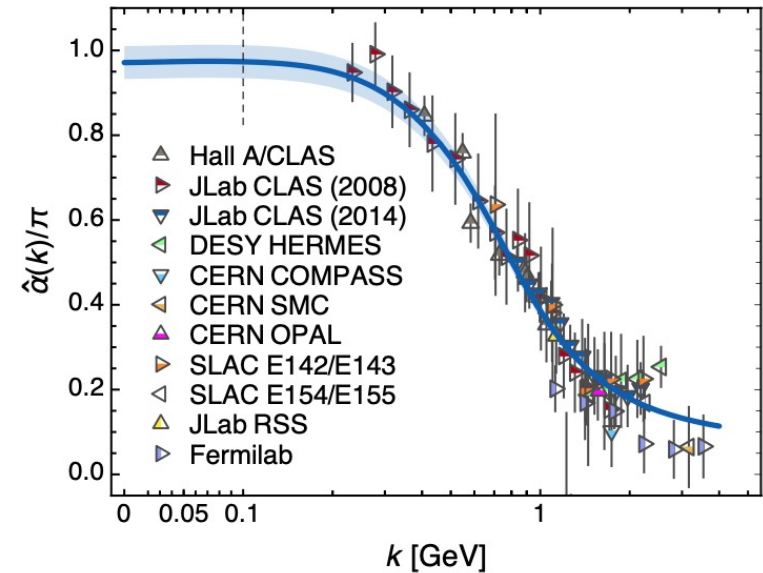


Basics for Insight into EHM: Continuum and Lattice QCD Synergy

Emergence of Dressed Quarks and Gluons D. Binosi et al., Phys. Rev. D 95, 031501 (2017)



QCD Running Coupling $\alpha(k)$ Zh-F. Cui et al., Chin. Phys. C44, 083102 (2020)

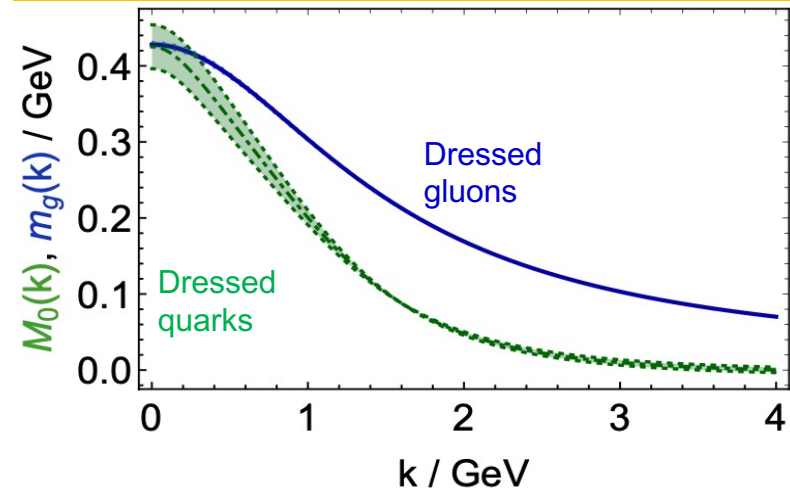


In the regime of the QCD running coupling comparable with unity, the dressed quarks and gluons with distance (momentum) dependent masses emerge from QCD, as follows from the equation of the motion for the QCD fields depicted above

Basics for Insight into EHM: Continuum and Lattice QCD Synergy

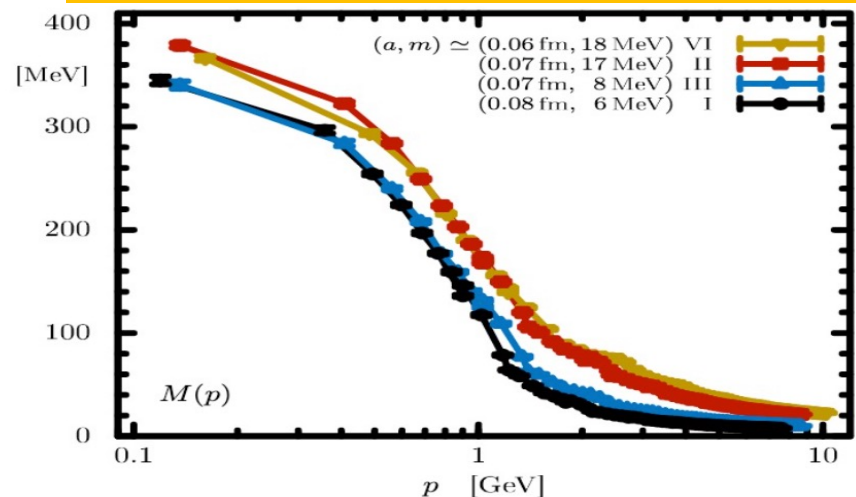
- Dressed quark/gluon masses converge at the complete QCD mass scale of $0.43(1)$ GeV - value impacted by Higgs mechanism.
- Express the fundamental feature: emergence of the quark and gluon masses even in the case of massless quarks in chiral limit and massless QCD gluons.
- Continuum QCD results get support from LQCD
- Insight into dressed quark mass function from data on hadron structure represents a challenge for experimental hadron physics

Dressed Quark/Gluon Masses (continuum QCD)
C.D. Roberts, Symmetry 12, 1468 (2020)



Inferred from QCD Lagrangian with only the Λ_{QCD} parameter

Dressed Quark Mass (lattice QCD)
O. Olivera et al., Phys. Rev. D 99, 094506 (2019)



Summary of Published CLAS Data on Exclusive Meson Electroproduction off Protons in N* Excitation Region

Hadronic final state	Covered W-range, GeV	Covered Q ² -range, GeV ²	Measured observables
π^+n	1.1-1.38 1.1-1.55 1.1-1.70 1.6-2.00	0.16-0.36 0.3-0.6 1.7-4.5 1.8-4.5	$d\sigma/d\Omega$ $d\sigma/d\Omega$ $d\sigma/d\Omega, A_b$ $d\sigma/d\Omega$
π^0p	1.1-1.38 1.1-1.68 1.1-1.39 1.1-1.80	0.16-0.36 0.4-1.8 3.0-6.0 0.4-1.0	$d\sigma/d\Omega$ $d\sigma/d\Omega, A_b, A_t, A_{bt}$ $d\sigma/d\Omega$ $d\sigma/d\Omega$
ηp	1.5-2.3	0.2-3.1	$d\sigma/d\Omega$
$K^+\Lambda$	thresh-2.6	1.40-3.90 0.70-5.40	$d\sigma/d\Omega$ P^0, P'
$K^+\Sigma^0$	thresh-2.6	1.40-3.90 0.70-5.4	$d\sigma/d\Omega$ P'
$\pi^+\pi^-p$	1.3-1.6 1.4-2.1 1.4-2.0	0.2-0.6 0.5-1.5 2.0-5.0	Nine 1-fold differential cross sections

- $d\sigma/d\Omega$ —CM angular distributions
- A_b, A_t, A_{bt} —longitudinal beam, target, and beam-target asymmetries
- P^0, P' —recoil and transferred polarization of strange baryon

Around 150,000 data points!

Almost full coverage of the final state hadron phase space

The measured observables from CLAS are stored in the CLAS Physics Data Base <http://clas.sinp.msu.ru/cgi-bin/jlab/db.cgi>



Approaches for Extraction of $\gamma_v N^*$ Electrocouplings from the CLAS Exclusive Meson Electroproduction Data

Analyses of different meson electroproduction channels independently:

➤ $\pi^+ n$ and $\pi^0 p$ channels:

Unitary Isobar Model (UIM) and Fixed-t Dispersion Relations (DR)

I.G. Aznauryan, Phys. Rev. C67, 015209 (2003)

I.G. Aznauryan et al. (CLAS), Phys. Rev. C80, 055203 (2009)

I.G. Aznauryan et al. (CLAS), Phys. Rev. C91, 045203 (2015)

➤ ηp channel:

Extension of UIM and DR

I.G. Aznauryan, Phys. Rev. C68, 065204 (2003)

Data fit at $W < 1.6$ GeV, assuming $N(1535)1/2^-$ dominance

H. Denizli et al. (CLAS), Phys. Rev. C76, 015204 (2007)

➤ $\pi^+ \pi^- p$ channel:

Data driven JLab-MSU meson-baryon model (JM)

V.I. Mokeev, V.D. Burkert et al., Phys. Rev. C80, 045212 (2009)

V.I. Mokeev et al. (CLAS), Phys. Rev. C86, 035203 (2012)

V.I. Mokeev, V.D. Burkert et al., Phys. Rev. C93, 054016 (2016)

Global coupled-channel analysis of $\gamma_{r,v} N$, πN , ηN , $\pi\pi N$, $K\Lambda$, $K\Sigma$ exclusive channels:

H. Kamano, Few Body Syst. 59, 24 (2018). Argonne-Osaka

H. Kamano, JPS Conf. Proc. 13, 010012 (2017). Argonne-Osaka

M. Mai et al., Phys. Rev. C103, 065204 (2021) Jülich-Bonn-Washington

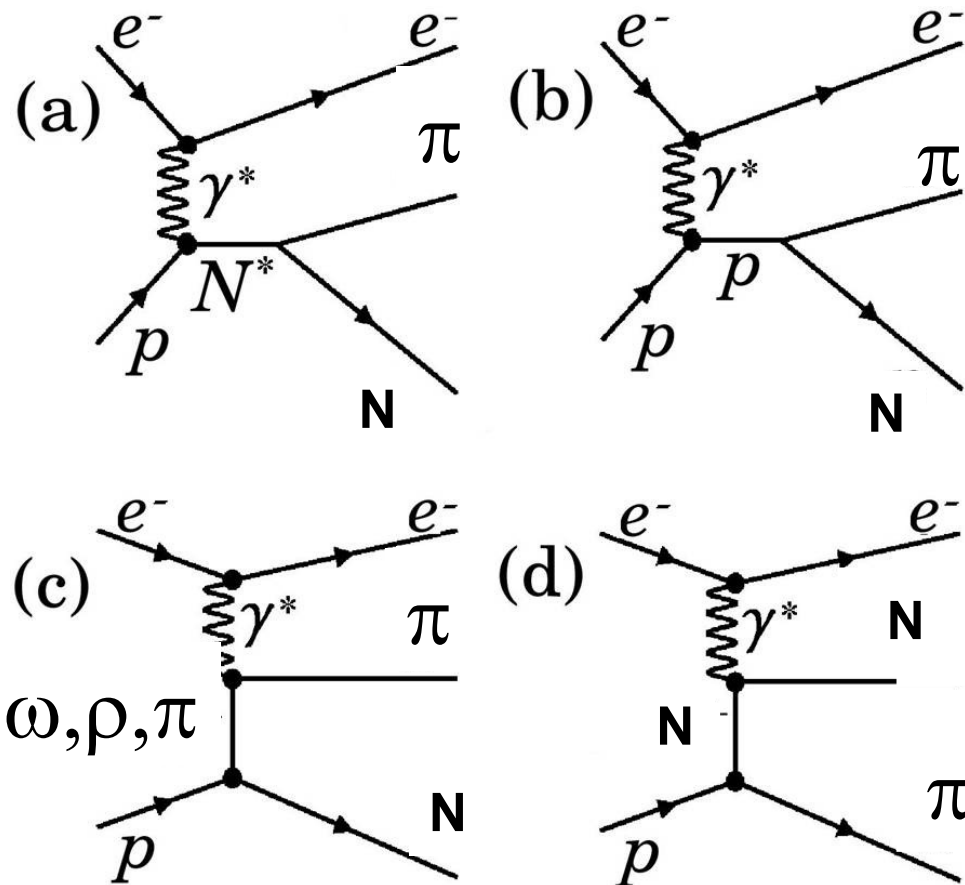


Approaches for the Extraction of $\gamma_{\nu p N^*}$ Electrocouplings from $N\pi$ Exclusive Electroproduction off Protons

The Model based on fixed- t Dispersion Relations (DR)

- the real parts of invariant $N\pi$ electroproduction amplitudes are computed from their imaginary parts employing fixed- t dispersion relations.
- the imaginary parts of the $N\pi$ electroproduction amplitudes at $W > 1.3$ GeV are saturated by the resonant parts and were computed from N^* parameters fit to the data.

Unitary Isobar Model (UIM)



I. G. Aznauryan, Phys. Rev. C67, 015209 (2003);

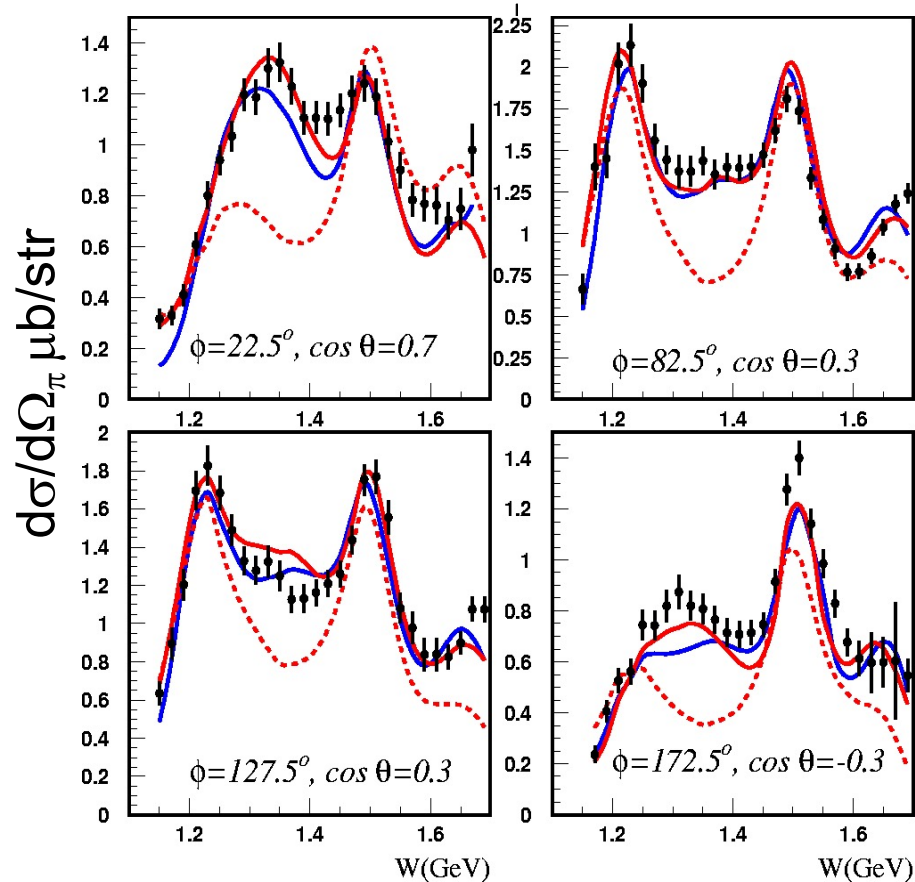
I.G.Aznauryan, V.D.Burkert, et al. (CLAS Collaboration), PRC 80, 055203 (2009).

Fits to $\gamma p \rightarrow \pi^+ n$ Differential Cross Sections

$Q^2 = 2.05 \text{ GeV}^2$

— DR
 DR w/o P11
 — UIM

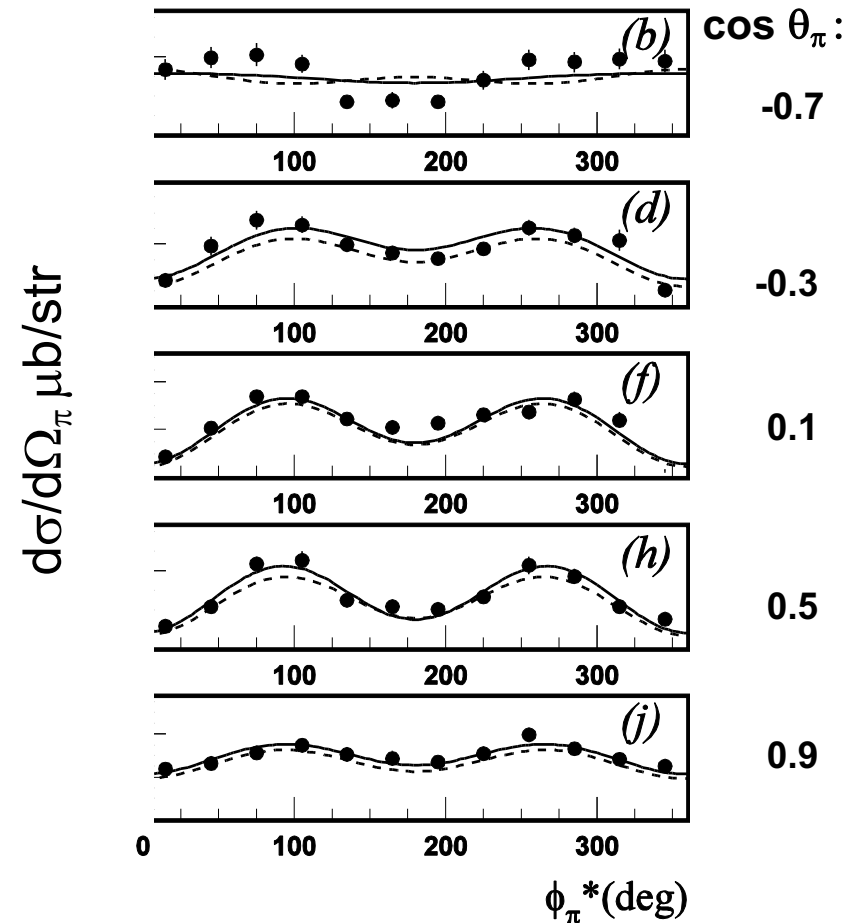
I.G. Aznauryan et al., Phys. Rev. C80, 055203 (2009).



$W = 1.68 \text{ GeV}$
 $Q^2 = 1.8 \text{ GeV}^2$

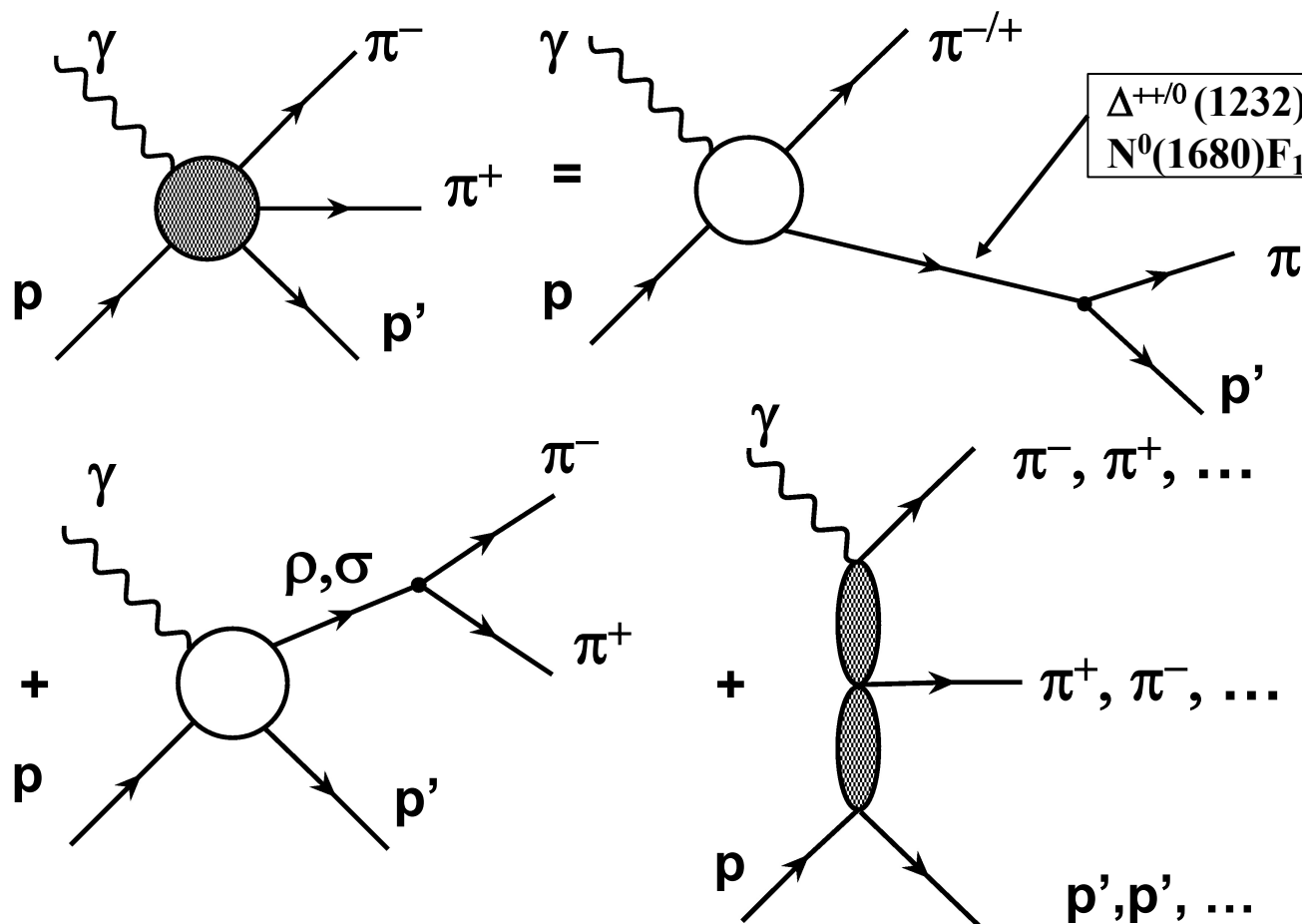
— DR
 UIM

K. Park et al., Phys. Rev. C91, 052014 (2015).



JM Model Analysis of the $\pi^+\pi^-p$ Photo-/Electroproduction

Major objectives: extraction of $\gamma_v p N^*$ electrocouplings and $\pi\Delta$, ρp decay widths



- six meson-baryon channels and direct $\pi^+\pi^-p$ production
- N^* contribute to $\pi\Delta$ and ρp channels only
- unitarized Breit-Wigner ansatz for resonant amplitudes

- V.I. Mokeev, V.D. Burkert, et al., (CLAS Collaboration) Phys. Rev. C86, 035203 (2012).
- V.I. Mokeev, V.D. Burkert, et al., Phys. Rev. C80, 045212 (2009).
- V.I. Mokeev, EPJ Web Conf. 241, 03002 (2020)

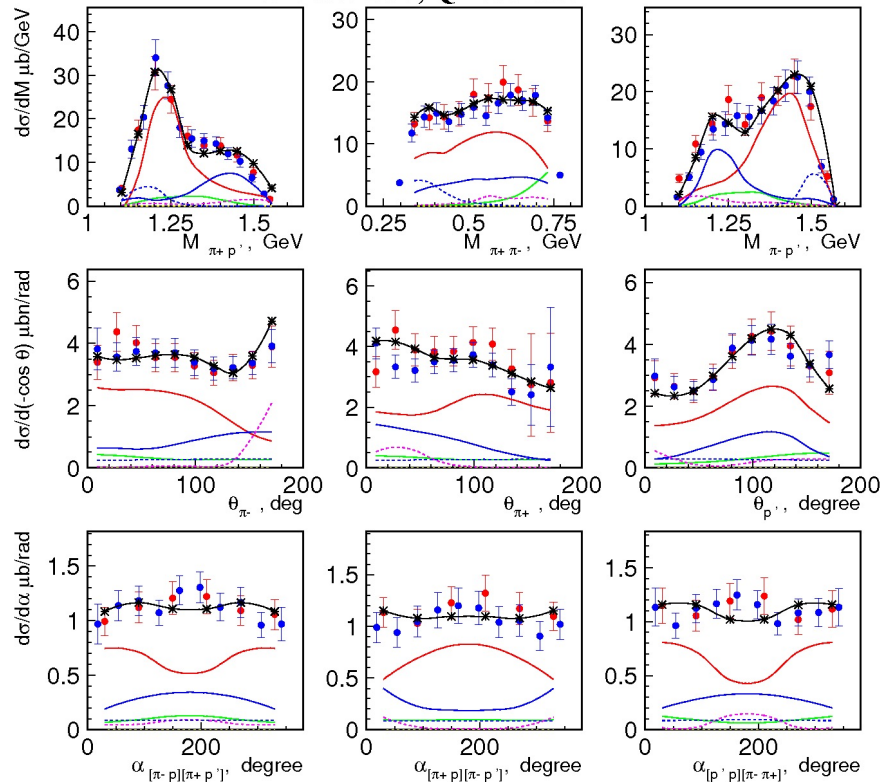
Accessing Resonance Electrocouplings from the $\pi^+\pi^-p$ Differential Electroproduction off Protons Cross Sections

Contributing mechanisms seen in the data

E. Isupov et al., CLAS Coll., Phys. Rev. C96, 025209 (2017)

A. Trivedi, Few Body Syst. 60, 5 (2019)

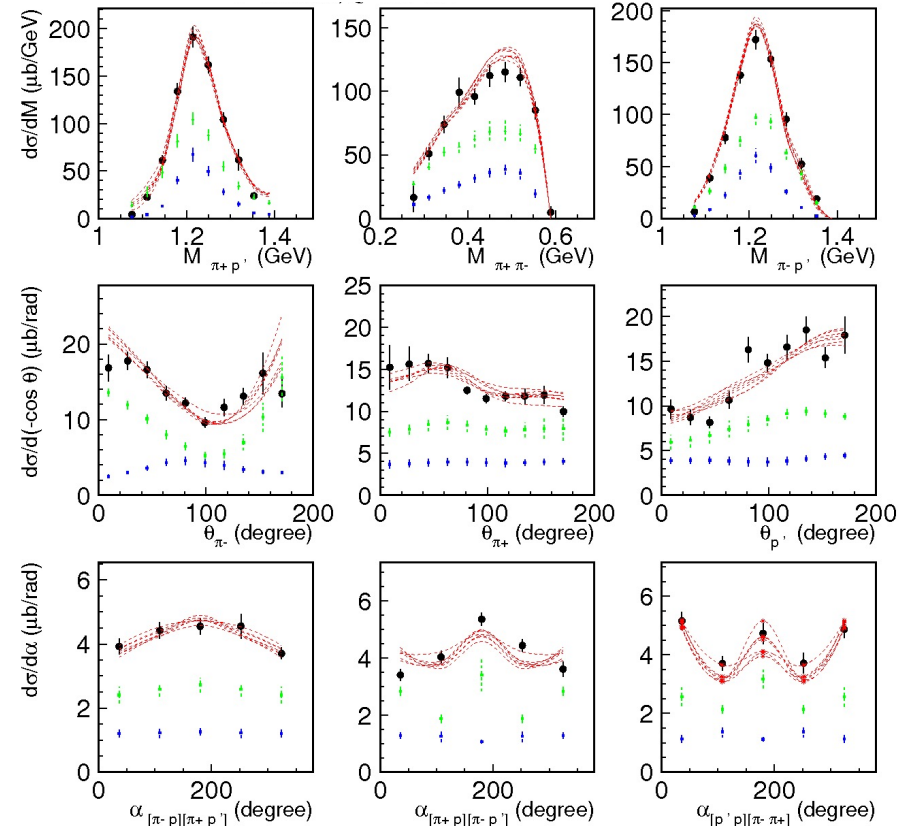
$W=1.71$ GeV, $Q^2=2.6$ GeV²



Resonant and non-resonant contributions

V.I. Mokeev, V.D. Burkert et al., Phys. Rev. C93, 054016 (2016).

$W=1.51$ GeV, $Q^2=0.65$ GeV²



full JM

$\rho\rho$

$\pi^+ N(1520)3/2^-$

$\pi^-\Delta^{++}$

$\pi^+\Delta^0$

$\pi^+ N(1680)5/2^+$

data fit within JM under variations of both resonant and background parameters

background cross sections

resonant cross sections

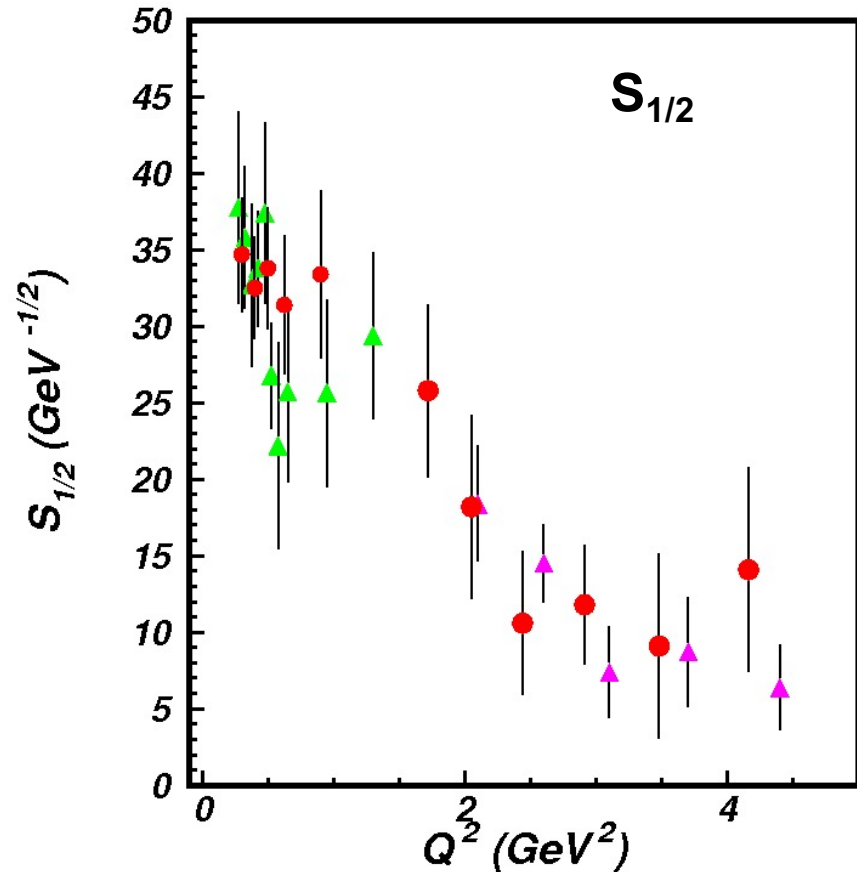
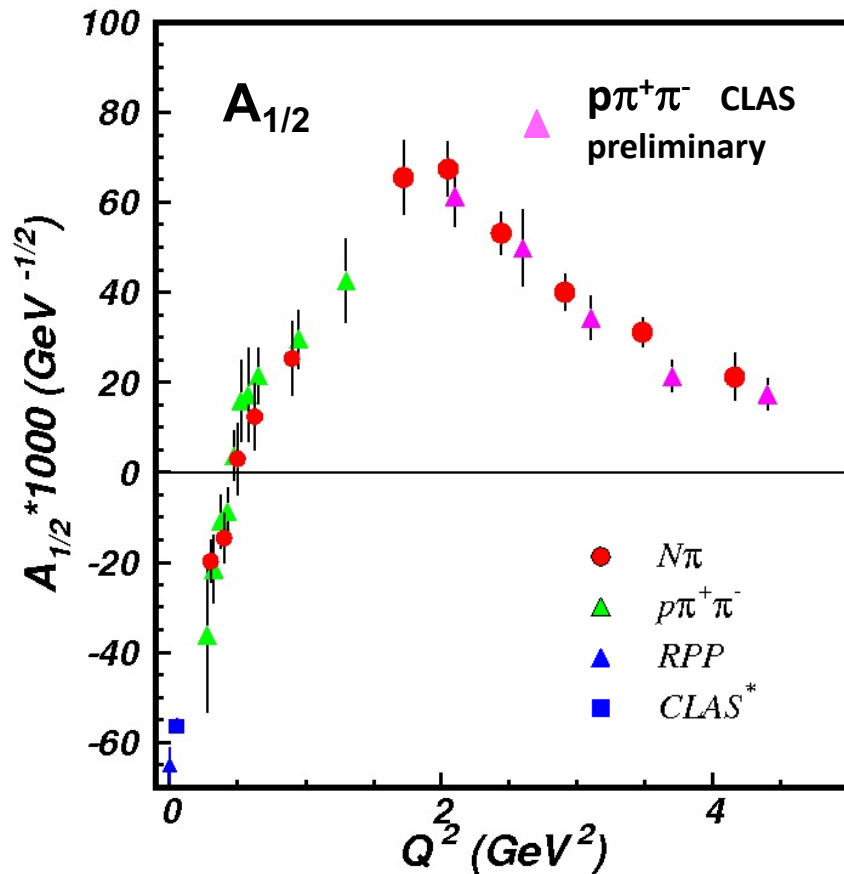


Nucleon Resonance Electrocouplings from Data On Exclusive Meson Electroproduction with CLAS

Exclusive meson electroproduction channels	Excited proton states	Q^2 -ranges for extracted $\gamma_{\nu}pN^*$ electrocouplings, GeV^2
$\pi^0 p, \pi^+ n$	$\Delta(1232)3/2^+$	0.16-6.0
	$N(1440)1/2^+, N(1520)3/2^-, N(1535)1/2^-$	0.30-4.16
$\pi^+ n$	$N(1675)5/2^-, N(1680)5/2^+, N(1710)1/2^+$	1.6-4.5
ηp	$N(1535)1/2^-$	0.2-2.9
$\pi^+ \pi^- p$	$N(1440)1/2^+, N(1520)3/2^-$	0.25-1.50
	$\Delta(1620)1/2^-, N(1650)1/2^-, N(1680)5/2^+, \Delta(1700)3/2^-, N(1720)3/2^+, N'(1720)3/2^+$	2.0-5.0 (preliminary) 0.5-1.5

- The N^* electroexcitation amplitudes ($\gamma_{\nu}pN^*$ electrocouplings) in a broad range of Q^2 offer a unique opportunity to explore universality on environmental sensitivity of dressed quark mass function.
- Consistent results on dressed quark mass function from $\gamma_{\nu}pN^*$ electrocouplings of different resonances validate insight into EHM in a nearly model-independent way.

Electrocouplings of $N(1440)1/2^+$ from πN and $\pi^+\pi^-p$ Electroproduction off Proton Data

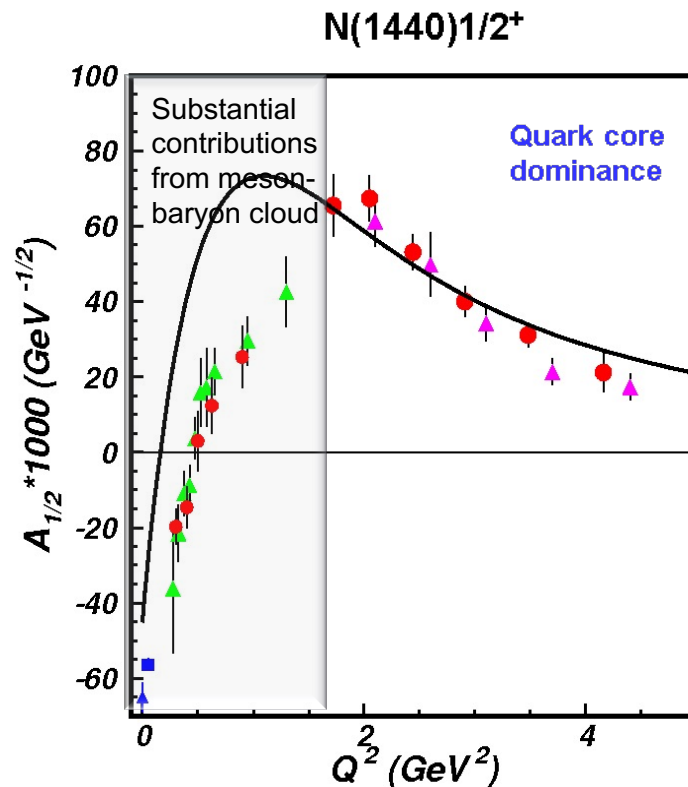
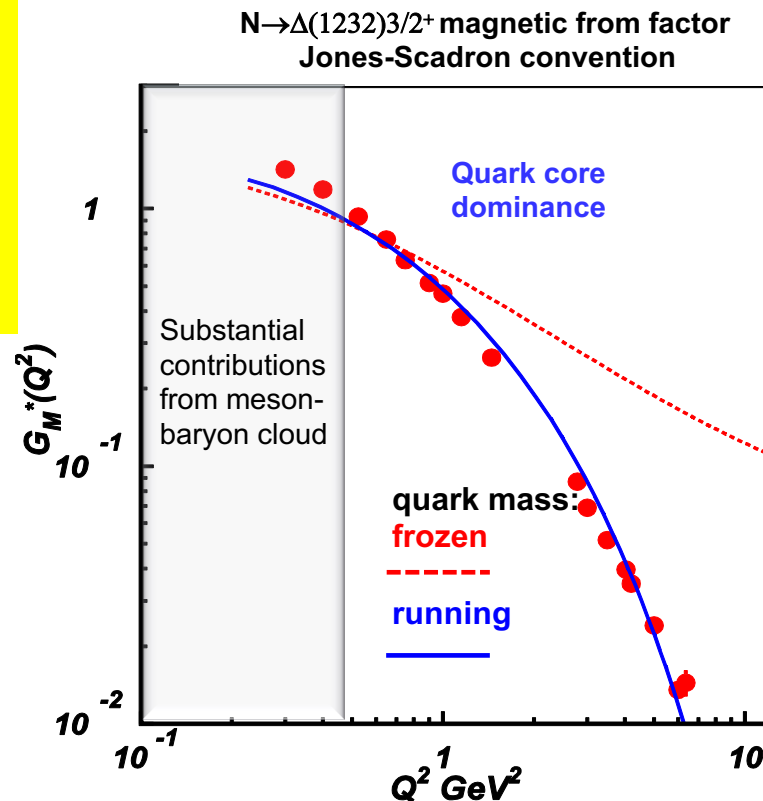


Consistent results on $N(1440)1/2^+$ electrocouplings from independent studies of two major πN and $\pi^+\pi^-p$ electroproduction channels with different non-resonant contributions allow us to evaluate the systematic uncertainties of these quantities in a nearly model-independent way

Insight to EHM From Resonance Electrocouplings

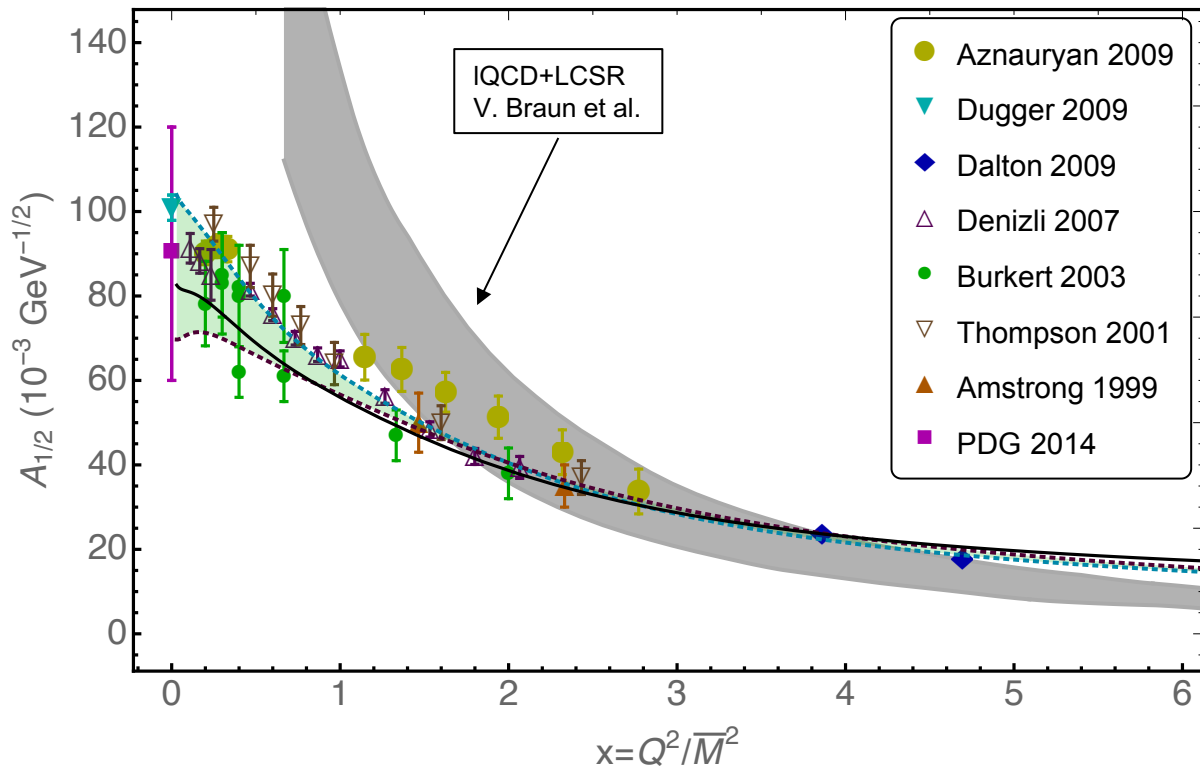
Dyson-Schwinger Equations (DSE):

- J. Segovia et al., PRL 115, 171801 (2015)
- J. Segovia et al., Few Body Syst. 55, 1185 (2014)



Good data description at $Q^2 > 2.0 \text{ GeV}^2$ achieved with the same dressed quark mass function for the ground and two excited nucleon states of distinctively different structure **validates the continuum QCD results on the momentum dependence of the dressed quark mass**. $\gamma_p N^*$ electrocoupling data offer access to the strong QCD dynamics underlying hadron mass generation.

One of the most important achievements in hadron physics of the last decade in synergistic efforts between experimentalists, phenomenologists, and theorists



Continuum QCD Breakthrough:
 $N(1535)1/2^-$ electrocouplings computed under a traceable connection to the QCD Lagrangian (green area).
 C.D Roberts et al, private communication

The first preliminary continuum QCD evaluation of electro-excitation amplitudes of the $[70,1]$ supermultiplet resonances ($L_{3q}=1$) with the same dressed quark mass mass function as used for the resonances with $L_{3q}=0$

Studies of electroexcitation amplitudes for the resonances in the second region suggest the universality of dressed quark mass function for the ground and different excited states of the nucleon including spin-isospin flip, the first radial, and the first orbital ($L_{3q}=1$) excitations

Interpretation of the Structure at $W \sim 1.7$ GeV in $\pi^+\pi^-p$ Electroproduction

M. Ripani et al., CLAS Collaboration
Phys. Rev. Lett. 91, 022002 (2003)

..... conventional states only, consistent with PDG 02

—— implementing $N'(1720)3/2^+$ candidate or only
conventional states with different $N(1720)3/2^+$ $N\pi\pi$
decays than in PDG 02

Two equally successful ways for the data description:

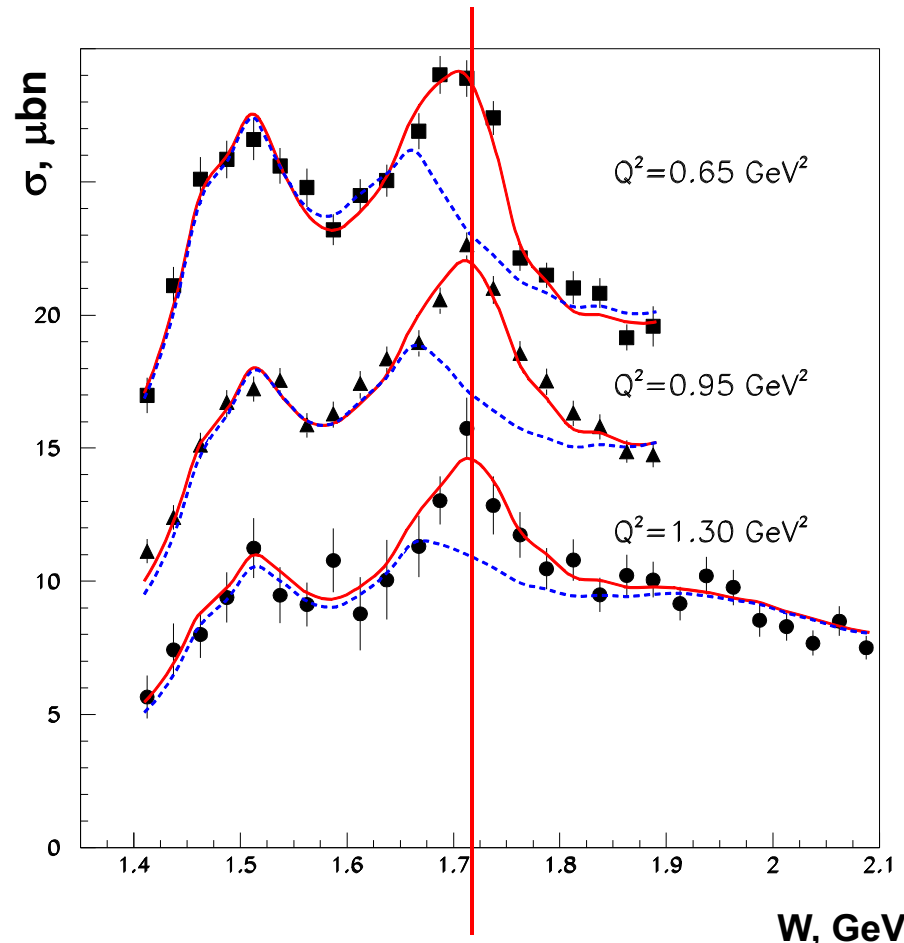
No new states, different than in PDG 02'

$N(1720)3/2^+$ $N\pi\pi$ hadronic decay widths:

	Γ_{tot} , MeV	BF($\pi\Delta$) %	BF($\rho\rho$) %
$N(1720)3/2^+$ decays fit to the CLAS $N\pi\pi$ data	126 ± 14	64-100	<5
$N(1720)3/2^+$ PDG 02'	150-300	<20	70-85

new $N'(1720)3/2^+$ and regular $N(1720)3/2^+$:

	Γ_{tot} , MeV	BF($\pi\Delta$) %	BF($\rho\rho$) %
$N'(1720)3/2^+$ New	119 ± 6	47-64	3-10.
$N(1720)3/2^+$ Conventional	112 ± 8	39-55	23-49



Evidence for the Existence of the New State $N'(1720)3/2^+$ from Combined $\pi^+\pi^-p$ Analyses in both Photo- and Electroproduction

V.I. Mokeev et al., Phys. Lett. B 805, 135457 (2020)

$N(1720)3/2^+$ hadronic decays from the CLAS data fit with conventional resonances only

	BF($\pi\Delta$), %	BF(ρp), %
electroproduction	64-100	<5
photoproduction	14-60	19-69

The contradictory BF values for $N(1720)3/2^+$ decays to the $\pi\Delta$ and ρp final states deduced from photo- and electroproduction data make it impossible to describe the data with conventional states only.

N^* hadronic decays from the data fit that incorporates the new $N'(1720)3/2^+$ state

Resonance	BF($\pi\Delta$), %	BF(ρp), %
$N'(1720)3/2^+$ electroproduction photoproduction	47-64 46-62	3-10 4-13
$N(1720)3/2^+$ electroproduction photoproduction	39-55 38-53	23-49 31-46
$\Delta(1700)3/2^-$ electroproduction photoproduction	77-95 78-93	3-5 3-6

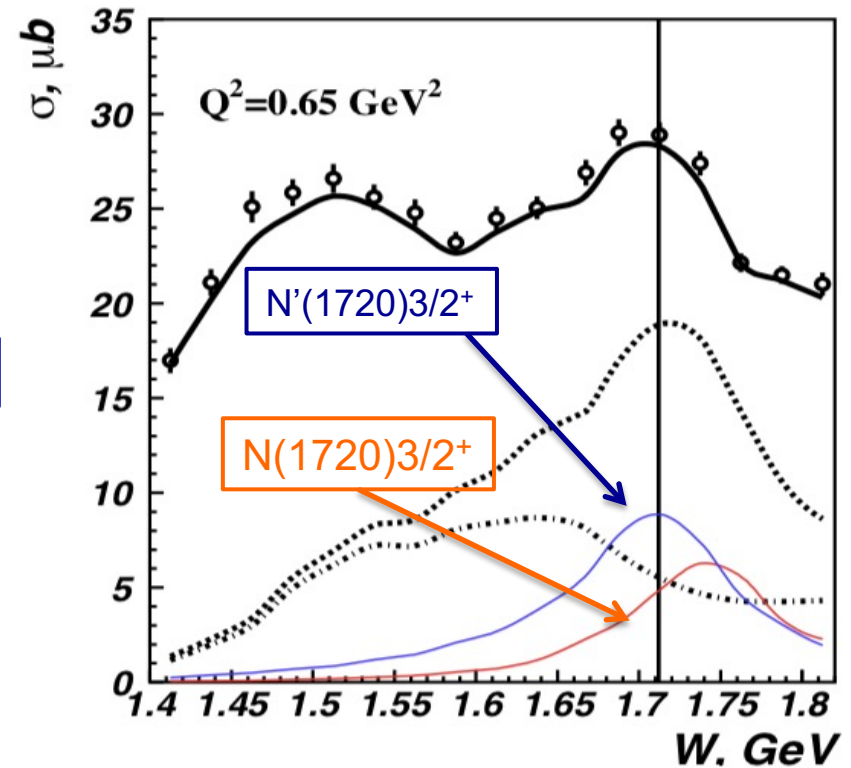
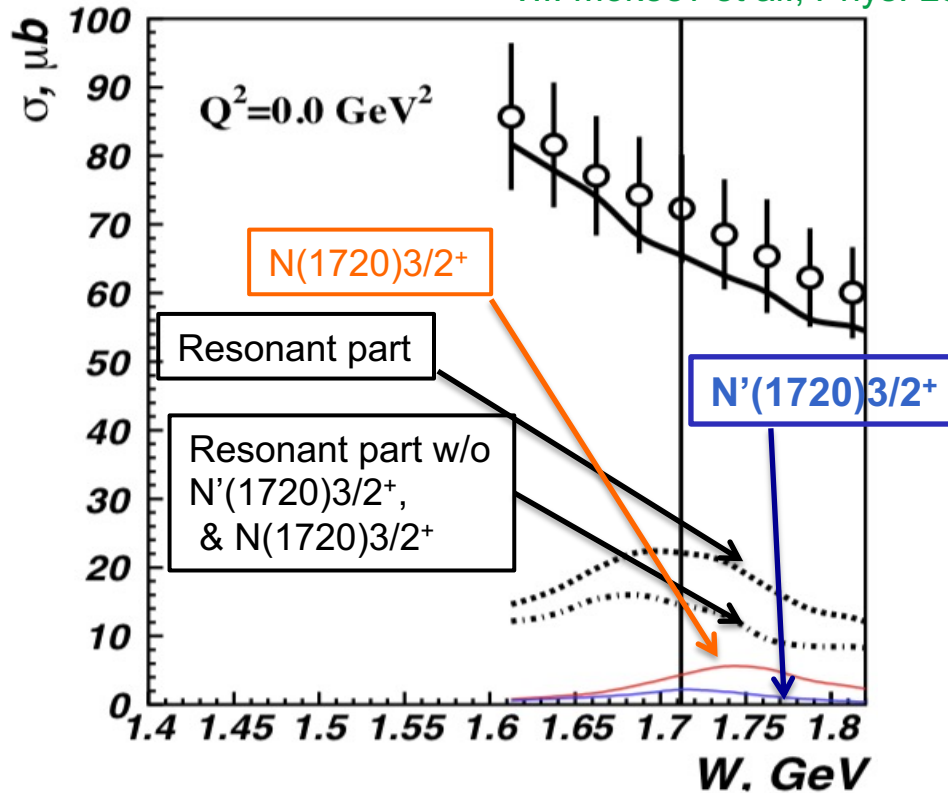
The successful description of the $\pi^+\pi^-p$ photo- and electroproduction data achieved by implementing new $N'(1720)3/2^+$ state with Q^2 -independent hadronic decay widths of all resonances contributing at $W \sim 1.7$ GeV provides strong evidence for the existence of the new $N'(1720)3/2^+$ state.

Newly Discovered $N'(1720) 3/2^+$

$\pi^+\pi^-p$ photoproduction

$\pi^+\pi^-p$ electroproduction

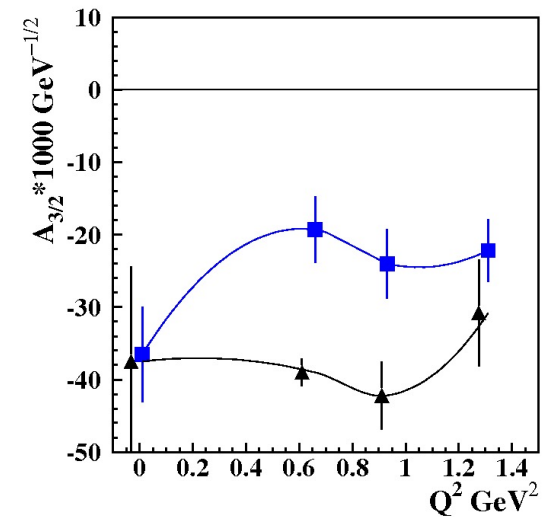
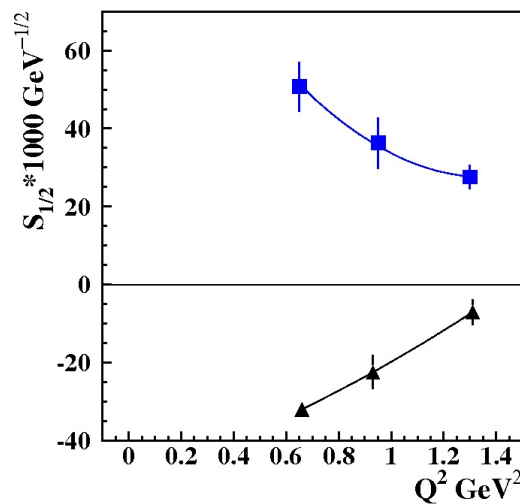
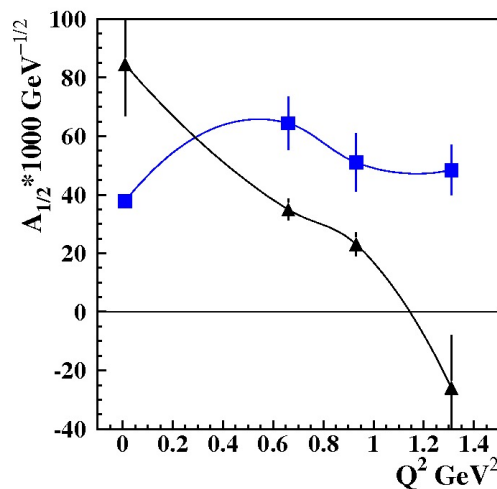
V.I. Mokeev et al., Phys. Lett. B 805, 135457 (2020)





- Evidence of a new $N'(1720) 3/2^+$ resonance from the combined analysis of CLAS photo- and electroproduction of the $\pi^+\pi^-p$ channel

The Parameters of the New N'(1720)3/2⁺ State from the CLAS Data Fit

The photo-/electrocouplings of the N'(1720)3/2⁺ and conventional N(1720)3/2⁺ states



 N'(1720)3/2⁺
 N(1720)3/2⁺

Resonance	Mass, GeV	Total width, MeV
N'(1720)3/2 ⁺	1.715-1.735	120±6
N(1720)3/2 ⁺	1.743-1.753	112±8

- N'(1720)3/2⁺ is the only new resonance for which data on electroexcitation amplitudes have become available.
- Gaining insight into the “missing” resonance structure will shed light on their peculiar structural features that have made them so elusive, as well as on the emergence of new resonances from QCD.

SU(6)-Assignment for $N'(1720)3/2^+$ and $N(1720)3/2^+$

New resonances discovered from exclusive meson photoproduction data revealed the following pattern of the high-lying resonance spectrum under approximate $SU(6) \times O(3)$ symmetry

$[70, 2^+]$ multiplet

$S_q=3/2$ $N(1880)1/2^+$ $N(1900)3/2^+$ $N(2000)5/2^+$ $N(2000)7/2^+$

$M_{\text{aver}}(S_q=3/2)=1.96 \text{ GeV}$. $\Delta M(S_q=3/2)=0.075 \text{ GeV}$

$S_q=1/2$ $N'(1720)3/2^+$ $N(1860)5/2^+$

$\Delta M(S_q=3/2-S_q=1/2)[70, 2^+]=\Delta M(S_q=3/2-S_q=1/2)[70, 1^-]=0.16 \text{ GeV}$

$M_{\text{aver}}(S_q=1/2)=M_{\text{aver}}(S_q=3/2)-\Delta M(S_q=3/2-S_q=1/2)[70, 2^+]=1.96-0.16=1.80 \text{ GeV}$

$M(N'(1720)3/2^+)=M_{\text{aver}}(S_q=1/2)-\Delta M(S_q=3/2)=1.80-0.075=1.73 \text{ GeV}$ consistent with the mass of $N'(1720)3/2^+$ inferred from the $\pi^+\pi^-p$ photo-/electroproduction data.

$N'(1720)3/2^+$: three constituent quarks of the total spin $S_q=1/2$ and of orbital momentum $L=2$ in $[70, 2^+]$ multiplet, double orbital excitation

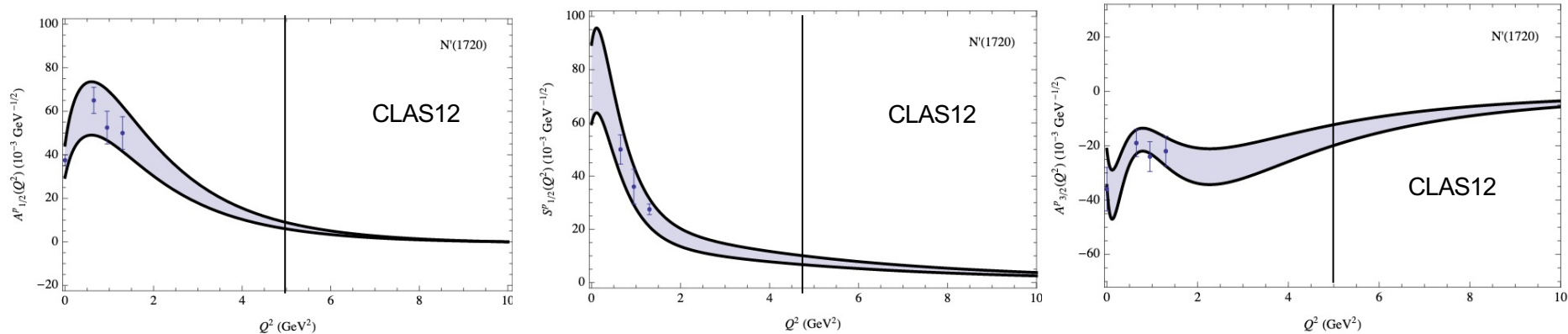
$N(1720)3/2^+$: three constituent quarks of the total spin $S_q=1/2$ and of orbital momentum $L=2$ in $[56, 2^+]$ multiplet

Quark model evaluation of $\gamma_{\nu p N^*}$ electrocouplings under the aforementioned assignments for $N(1720)3/2^+$ and $N'(1720)3/2^+$ states will shed light on peculiar features in $N'(1720)3/2^+$ structure



Insight into the Structure of the New $N'(1720)3/2^+$

Soft wall Ads/CFT, V.E. Lyubovitskij and I. Schmidt, e-Print:2009.07115 [hep--ph]

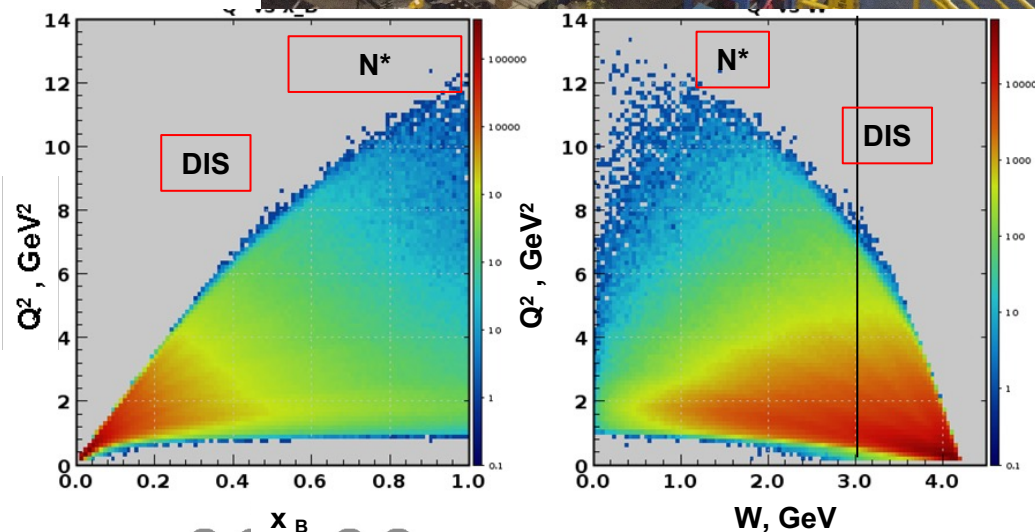
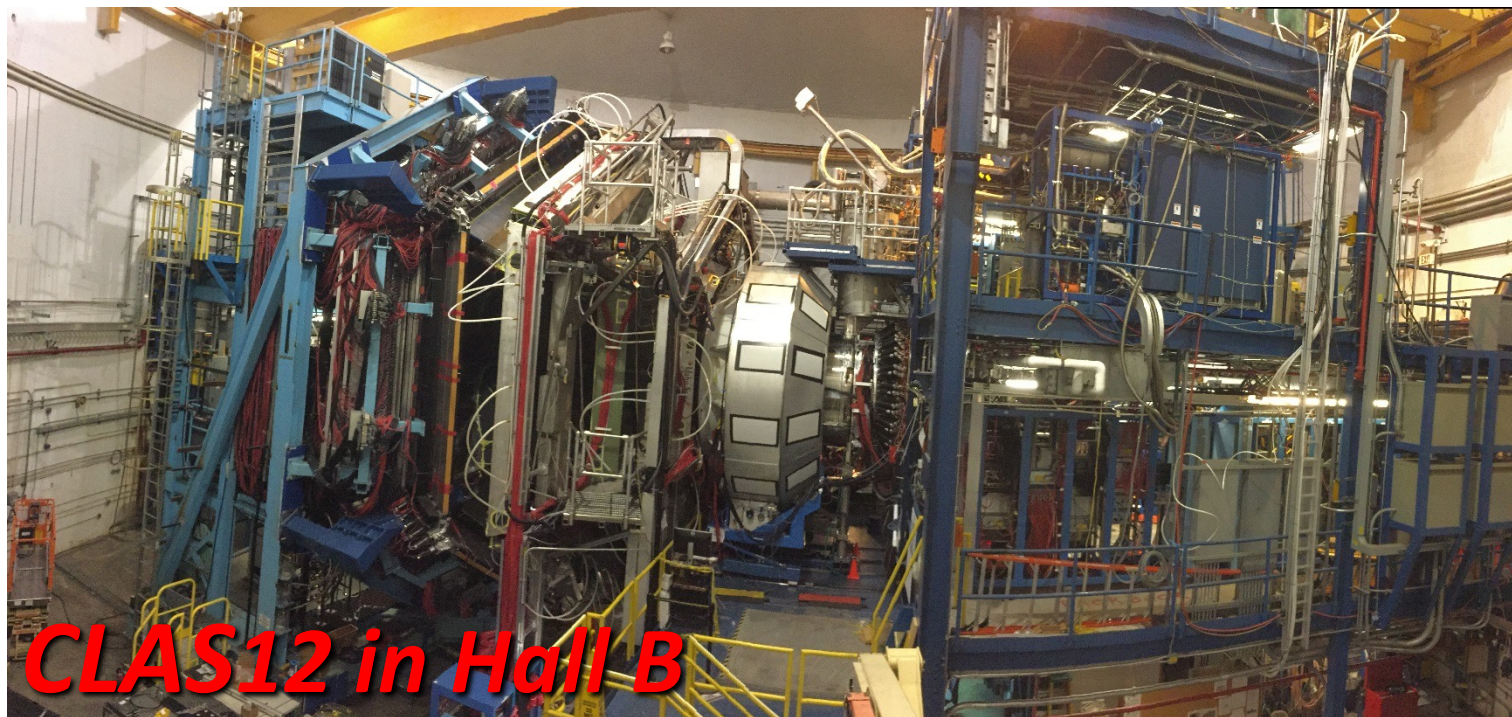


$N \rightarrow N(1720)$	$g_{35}^{2A} = -11.58, g_{46}^{2A} = 34.50, g_{57}^{2A} = -22.60, g_{35}^{1B} = 79.15, g_{46}^{1B} = 67.11, g_{57}^{1B} = 29.95,$ $g_{35}^{1C} = -36.53, g_{46}^{1C} = 105.65, g_{57}^{1C} = -58.59, g_{35}^{1D} = 0.16, g_{46}^{1D} = -0.47, g_{57}^{1D} = 0.31,$ $g_{35}^{2E} = 12.14, g_{46}^{2E} = 10.29, g_{57}^{2E} = 4.59, g_{35}^{2F} = 5.56, g_{46}^{2F} = -16.07, g_{57}^{2F} = 8.91$
$N \rightarrow N'(1720)$	$g_{35}^{2A} = 30.18, g_{46}^{2A} = -54.02, g_{57}^{2A} = 24.82, g_{35}^{1B} = -1.15, g_{46}^{1B} = 6.41, g_{57}^{1B} = -2.87,$ $g_{35}^{1C} = -17.77, g_{46}^{1C} = 107.19, g_{57}^{1C} = -62.71, g_{35}^{1D} = 8.48, g_{46}^{1D} = -15.18, g_{57}^{1D} = 6.97,$ $g_{35}^{2E} = -0.60, g_{46}^{2E} = 3.37, g_{57}^{2E} = -1.51, g_{35}^{2F} = -3.57, g_{46}^{2F} = 21.56, g_{57}^{2F} = -12.61$

Leading/sub-leading contributions into $N'(1720)3/2^+$ and $N(1720)3/2^+$ are coming from the same/different AdS fields

- Checking $[70,2^+]$ and $[56,2^+]$ assignments for $N'(1720)3/2^+$ and $N(1720)3/2^+$, respectively (R.Bijker et al., PRD94, 074040 (2016), G.Ramalho, Few Body Syst. 59, 92 (2018)) from the results on $\gamma_p n^*$ electrocouplings. If confirmed, discovery of $N'(1720)3/2^+$ represents the first observation of the resonance with two non-zero orbital momenta l_λ and l_ρ in three quark system.
- Alternative assignment of $N'(1720)3/2^+$ as a member of 27-SU(3) baryon multiplet of chiral soliton model (G.-S. Yang and H.-C. Kim, PTEP, 093D01 (2019))

12 GeV Era with the CLAS12 Detector

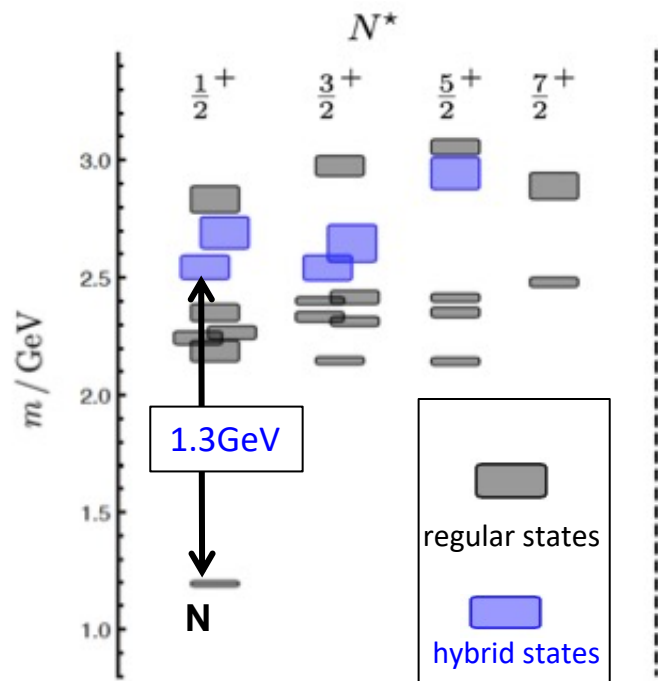


Physics run started successfully
in February 2018

Hunting for Glue in Excited Baryons with CLAS12

Can glue be a structural component to generate hybrid q^3g baryon states?

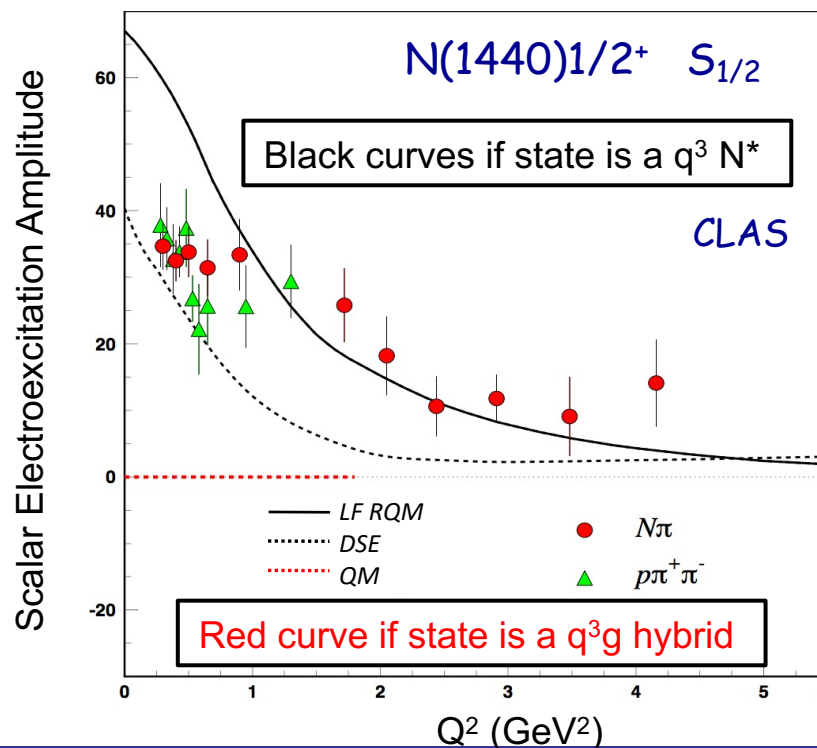
Predictions of the N^* spectrum from QCD show both regular q^3 and hybrid q^3g states



JLab LQCD group results

Search for hybrid baryons with CLAS12 in exclusive KY and $\pi^+\pi^-p$ electroproduction

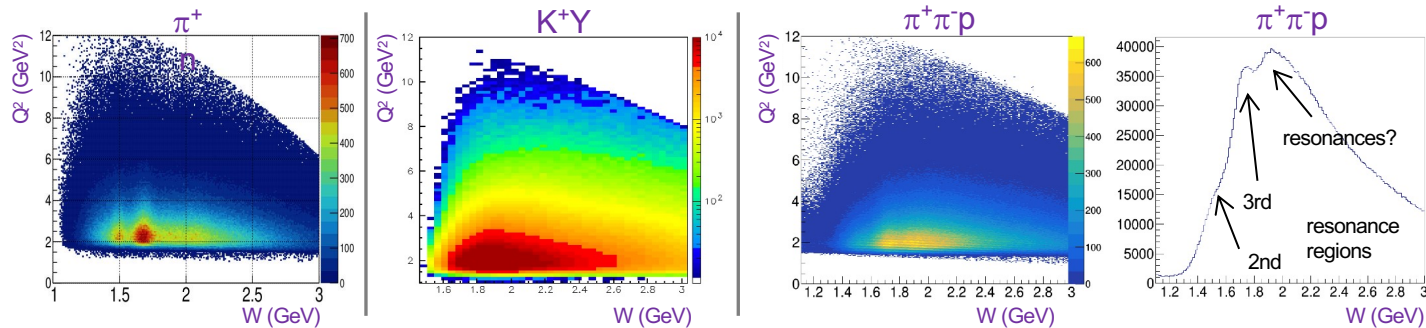
LQCD and/or QM predictions on Q^2 evolution of the hybrid-baryon electroexcitation amplitudes are critical in order to establish the nature of a baryon state



N* Electroexcitation to high Q² with CLAS12

Expected outcome: The first results on the $\gamma_p N^*$ electrocouplings of most N* states from data in the range $W < 3.0$ GeV and $Q^2 > 5.0$ GeV² for exclusive reaction channels: πN , $\pi\pi N$, KY , K^*Y , KY^*

kinematic coverage for RG-A data @ 10.6 GeV



Expected events per Q²/W bin for full RG-A dataset

π^+n			$K^+\Lambda$ & $K^+\Sigma^0$					$\pi^+\pi p$		
Q ² [GeV ²]	W [GeV] 1.5-1.55	W [GeV] 1.7-1.75	Q ² [GeV ²]	W _Λ [GeV] 1.7-1.75	W _Σ [GeV] 1.7-1.75	W _Λ [GeV] 1.9-1.95	W _Σ [GeV] 1.9-1.95	Q ² [GeV ²]	W [GeV] 1.7-1.75	W [GeV] 1.9-1.95
			1.4-2.2	63417	6012	66564	33170			
			2.2-3.0	72144	5364	77443	28720			
5.2-5.8	15272	4175	3.0-4.0	52358	3945	51991	18936	5.2-5.8	2813	2808
5.8-6.5	10737	2637	4.0-5.0	24833	3103	26690	5925	5.8-6.5	1822	1969
6.5-7.2	7367	1684	5.0-6.0	11203	1598	11160	2642	6.5-7.2	1159	1294
7.2-8.1	4567	1290	6.0-7.0	5566	648	6300	943	7.2-8.1	661	924
8.1-9.1	2742	540	7.0-8.0	2606	338	3276	633	8.1-9.1	364	414
9.1-10.5	1453	194	8.0-9.0	1440	244	936	86	9.1-10.5	118	179

Collecting the remainder of the approved RG-A beam time will give a factor of two more statistics

This will extend the Q² range of the $\gamma_p N^*$ electrocouplings to **8-10 GeV²** for each of these channels – *the data collected so far will limit us to 6-8 GeV²*



Emergence of Hadron Mass and Quark-Gluon Confinement

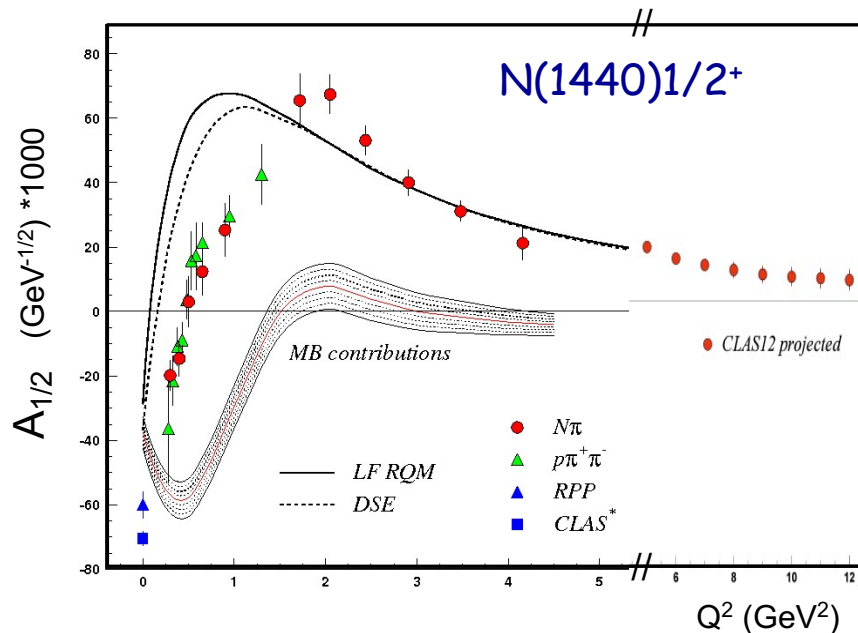
N* electroexcitation studies at JLab during **and after 12 GeV era** will address the critical questions:

How is >98% of visible mass generated?

How does confinement emerge from QCD and how is it related to Dynamical Chiral Symmetry Breaking?

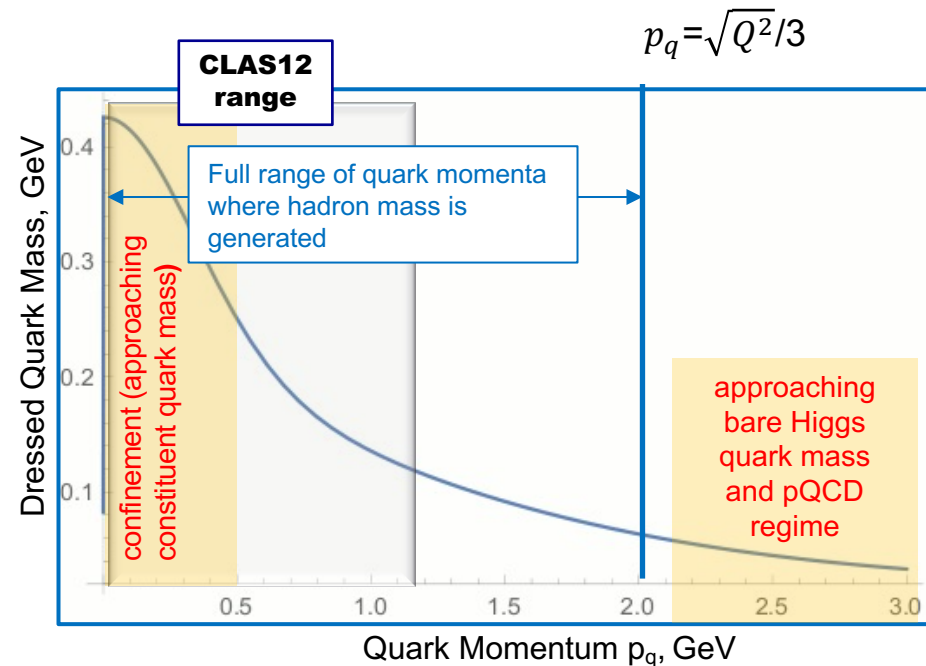
(S.J, Brodsky et al., Int. J. Mod. Phys. Rev. E29, 2030006 (2020))

Mapping-out quark mass function from the results on $\gamma_v p N^*$ electrocouplings of spin-isospin flip, radial, and orbital excited nucleon resonances at $5 < Q^2 < 36 \text{ GeV}^2$ is needed to explore the full range of distances where the dominant part of hadron mass is generated



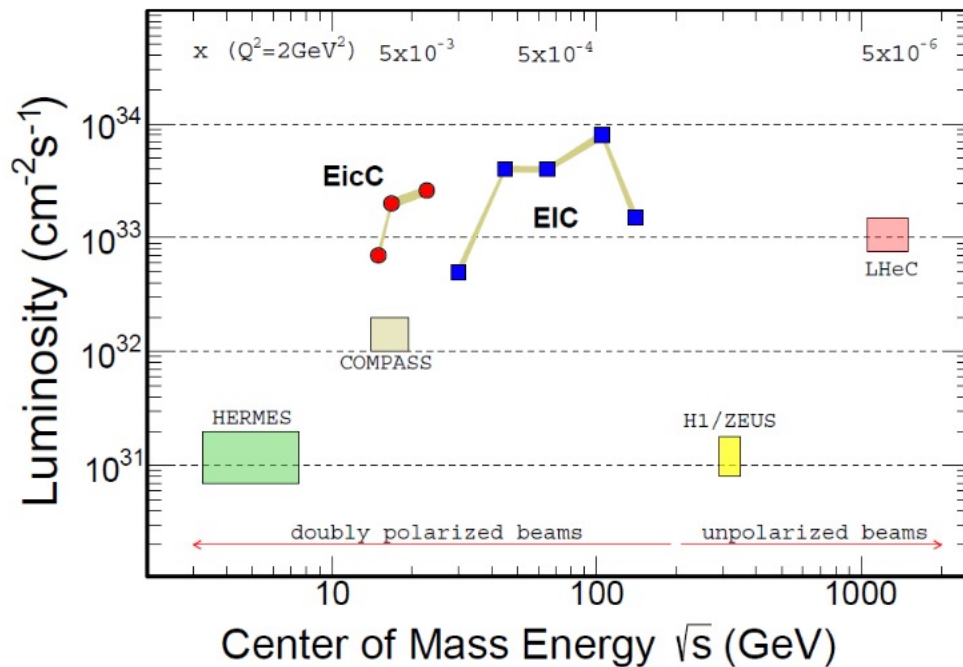
CLAS results vs. theory expectations with running quark mass

Access to the dressed quark/hadron mass generation



Studies of $\gamma_p N^*$ Electrocouplings at $Q^2 > 10 \text{ GeV}^2$

Energy and luminosity increase up to $>10^{36} \text{ cm}^{-2}\text{s}^{-1}$ are needed in order to obtain information on the $\gamma_p N^*$ electrocouplings at $Q^2 > 10 \text{ GeV}^2$, allowing us to map out the momentum dependence of the dressed quark mass within the entire range of distances where the dominant part of hadron mass is generated



Both EicC and EIC would need much higher, unlikely feasible luminosity

The exclusive electroproduction measurements foreseen at JLab after completion of the 12 GeV program:

- Beam energy at fixed target: 24 GeV
- Nearly 4π coverage
- High luminosity



Offer maximal achievable luminosity for extraction of $\gamma_p N^*$ electrocouplings at $Q^2 > 10 \text{ GeV}^2$

Conclusions and Outlook

- Studies of exclusive meson photoproduction in the resonance region provided precise results on differential cross sections and polarization observables for most exclusive photoproduction channels. Progress in the amplitude analyses allows us to establish the masses, total/partial hadronic decay widths, and photocouplings for prominent resonances in the mass range <2.5 GeV. Further efforts are needed to improve agreement between N^* -parameters available from different analysis approaches.
- Several long-time awaited new baryon states (previous “missing” resonances) have been discovered in global multi-channel analyses of exclusive meson photo- and hadroproduction data with a major impact from the CLAS $K\Lambda$, $K\Sigma$ photoproduction data.
- New $N'(1720)3/2^+$ resonance has been observed in combined studies of $\pi^+\pi^-p$ photo- and electroproduction data measured with CLAS. Currently, it is the only “missing” resonance for which the results on Q^2 -evolution of $\gamma_v p N^*$ electrocouplings have become available allowing us to gain insight into the structure of new baryon states.
- The experiments of 12 GeV era at JLab and at EU, Asian facilities will complete studies of the excited nucleon state spectrum, including the search for hybrid baryons offering an insight into strong interaction dynamics which underlies the N^* -spectrum generation addressing: approximate symmetries for strong QCD regime, emergence of hadrons in early Universe, dual role of gluons as the strong force carriers and hadron matter constituents.

Conclusions and Outlook

- **CLAS detector provided the dominant part of the data on most exclusive meson electroproduction channels in the resonance region.** High-quality meson electroproduction data from CLAS have allowed us to determine the electrocouplings of most resonances in the mass range up to 1.8 GeV with consistent results from analyses of π^+n , π^0p , ηp , and $\pi^+\pi^-p$ electroproduction channels. **Resonance electrocouplings will become available for N^* in the mass range <2.0 GeV and at $Q^2 < 5.0$ GeV² (CLAS) and at $Q^2 < 10$ GeV² (CLAS12).**
- **Profound impact on the exploration of the emergence of hadron mass:**
A good description of CLAS results on $\Delta(1232)3/2^+$, $N(1440)1/2^+$, and $N(1535)1/2^-$ electroexcitation amplitudes achieved with the same dressed quark mass function as used previously in successful evaluations of the elastic ground nucleon and pion form factors, validate insight to the dynamics of hadron mass generation in a nearly model-independent way.
- **CLAS12 is the only facility in the world capable of obtaining the electrocouplings of all prominent N^* states at still unexplored ranges of low photon virtualities down to 0.05 GeV² and highest photon virtualities for exclusive reactions from 5.0 GeV² to 12 GeV² from measurements of $N\pi$, $\pi^+\pi^-p$, and KY electroproduction.**
- **The expected results will allow us:**
 - a) to search for hybrid-baryons and complete the N^* -spectrum exploration;
 - b) to map out the dressed quark mass function at the distances where the transition from quark-gluon confinement to pQCD regime is expected,
addressing the most challenging problems of the Standard Model on the nature of $>98\%$ of hadron mass and of quark-gluon confinement.

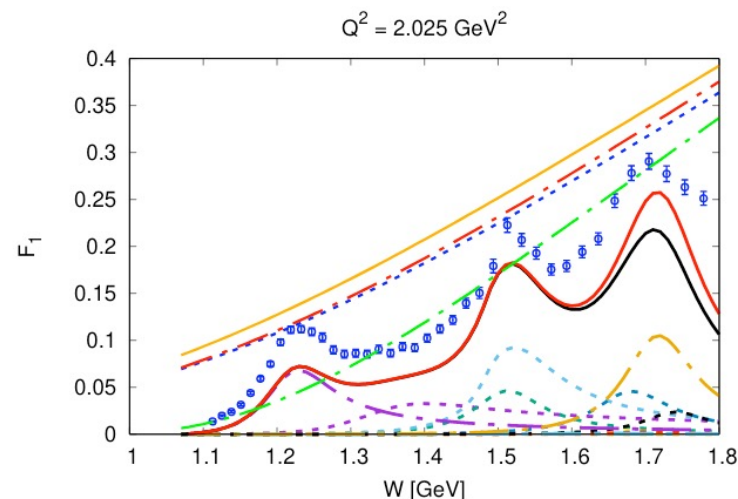
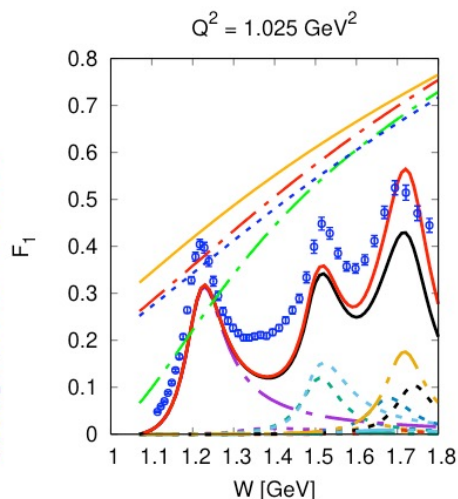
Back up

Resonant Contributions into Inclusive $F_1(W, Q^2)$ Structure Functions & the Contributions from the PDF in the Ground State of the Nucleon Evaluated from the Data in DIS Region

Resonant contributions:

A.N. Hiller Blin et al.,
PRC 100, 035201 (2019)

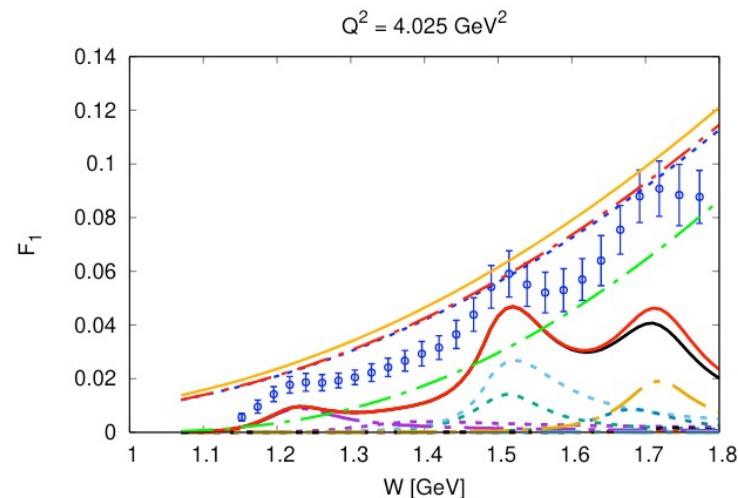
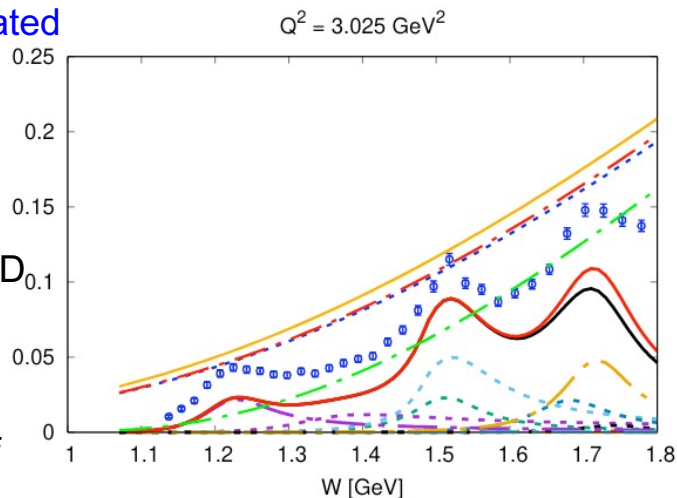
$N(1440) 1/2^+$
 $N(1520) 3/2^-$
 $N(1535) 1/2^-$
 $N(1650) 1/2^-$
 $N(1675) 5/2^-$
 $N(1680) 5/2^+$
 $N(1710) 1/2^+$
 $N(1720) 3/2^+$
 $\Delta(1232) 3/2^+$
 $\Delta(1620) 1/2^-$
 $\Delta(1700) 3/2^-$
 $N^*(1720) 3/2^+$
 Total
 Total coherent
 CLAS Data
 JAM
 JAM TMC Moffat
 JAM TMC Brady approx.
 JAM TMC Brady



Data points are from
interpolation of the
CLAS results re-evaluated
with the σ_L/σ_T ratio
from Hall C data

CLAS data:
M. Osipenko et al., PRD
67, 092001 (2003)

Hall C data:
Y. Liang, PhD thesis of
American University
(2003)



Green dot-dashed lines: F_1 from JAM PDF

Other smooth curves: F_1 from JAM PDF after target mass corrections within different prescriptions



N* studies at $0.05 \text{ GeV}^2 < Q^2 < 7.0 \text{ GeV}^2$ with CLAS12

Hybrid Baryons E12-16-010	Search for hybrid baryons (qqqq) focusing on $0.05 \text{ GeV}^2 < Q^2 < 2.0 \text{ GeV}^2$ in mass range from 1.8 to 3 GeV in $K\Lambda$, $N\pi\pi$, $N\pi$ (<i>A. D'Angelo, et al.</i>)
KY Electroproduction E12-16-010A	Study N* structure for states that couple to KY through measurements of cross sections and polarization observables that will yield Q^2 evolution of electrocoupling amplitudes at $Q^2 < 7.0 \text{ GeV}^2$ (<i>D. Carman, et al.</i>)

Approved by PAC44

Run Group conditions:

$E_b = 6.6 \text{ GeV}$, 50 days

$E_b = 8.8 \text{ GeV}$, 50 days

- Polarized electrons, unpolarized LH_2 target
- $L = 1 \times 10^{35} \text{ cm}^{-2}\text{s}^{-1}$